that regulates T cell differentiation by conditioning dendritic cell maturation. *Annu. Rev. Immunol.* 25: 193–219.
16. Ziegler, S. F., and D. Artis. 2010. Sensing the outside world: TSLP regulates barrier immunity. *Nat. Immunol.* 11: 289–293.
17. Blázquez, A. B., L. Mayer, and M. C. Berin. 2010. Thymic stromal lymphopoietin is required for gastrointestinal allergy but not oral tolerance. *Gastroenterology* 139: 1301–1309.
18. Rothenberg, M. E., J. M. Spergel, J. D. Sherrill, K. Annaiah, L. J. Martin, A. Cianferoni, L. Gober, C. Kim, J. Glessner, E. Frackelton, et al. 2010. Common variants at 5q22 associate with pediatric eosinophilic esophagitis. *Nat. Genet.* 42: 289–291.
19. Sherrill, J. D., P. S. Gao, E. M. Stucke, C. Blanchard, M. H. Collins, P. E. Putnam, J. P. Franciosi, J. P. Kushner, J. P. Abonia, A. H. Assa'ad, et al. 2010. Variants of thymic stromal lymphopoietin and its receptor associate with eosinophilic esophagitis. *J. Allergy Clin. Immunol.* 126: 160–165.e3.
20. Zaph, C., A. E. Troy, B. C. Taylor, L. D. Berman-Booty, K. J. Guild, Y. Du, E. A. Yost, A. D. Gruber, M. J. May, F. R. Greten, et al. 2007. Epithelial-cell-intrinsic IKK-beta expression regulates intestinal immune homeostasis. *Nature* 446: 552–556.
21. Taylor, B. C., C. Zaph, A. E. Troy, Y. Du, K. J. Guild, M. R. Comeau, and D. Artis. 2009. TSLP regulates intestinal immunity and inflammation in mouse models of helminth infection and colitis. *J. Exp. Med.* 206: 655–667.
22. Carpino, N., W. E. Thierfelder, M. S. Chang, C. Saris, S. J. Turner, S. F. Ziegler, and J. N. Ihle. 2004. Absence of an essential role for thymic stromal lymphopoietin receptor in murine B-cell development. *Mol. Cell. Biol.* 24: 2584–2592.
23. Zhou, B., M. R. Comeau, T. De Smedt, H. D. Liggitt, M. E. Dahl, D. B. Lewis, D. Gyarmati, T. Aye, D. J. Campbell, and S. F. Ziegler. 2005. Thymic stromal lymphopoietin as a key initiator of allergic airway inflammation in mice. *Nat. Immunol.* 6: 1047–1053.
24. Uchida, K., K. Okazaki, A. Debrecceni, T. Nishi, H. Iwano, M. Inai, S. Uose, H. Nakase, M. Ohana, C. Oshima, et al. 2001. Analysis of cytokines in the early development of gastric secondary lymphoid follicles in *Helicobacter pylori*-infected BALB/c mice with neonatal thymectomy. *Infect. Immun.* 69: 6749–6754.
25. Kido, M., N. Watanabe, T. Okazaki, T. Akamatsu, J. Tanaka, K. Saga, A. Nishio, T. Honjo, and T. Chiba. 2008. Fatal autoimmune hepatitis induced by concurrent loss of naturally arising regulatory T cells and PD-1-mediated signaling. *Gastroenterology* 135: 1333–1343.
26. Ohana, M., K. Okazaki, C. Oshima, K. Kawasaki, T. Fukui, H. Tamaki, M. Matsuura, M. Asada, T. Nishi, K. Uchida, et al. 2003. Inhibitory effects of *Helicobacter pylori* infection on murine autoimmune gastritis. *Gut* 52: 1102–1110.
27. Kido, M., J. Tanaka, N. Aoki, S. Iwamoto, H. Nishiura, T. Chiba, and N. Watanabe. 2010. *Helicobacter pylori* promotes the production of thymic stromal lymphopoietin by gastric epithelial cells and induces dendritic cell-mediated inflammatory Th2 responses. *Infect. Immun.* 78: 108–114.
28. Alderuccio, F., B. H. Toh, P. A. Gleeson, and I. R. Van Driel. 1995. A novel method for isolating monónuclear cells from the stomachs of mice with experimental autoimmune gastritis. *Autoimmunity* 21: 215–221.
29. Scheinecker, C., R. McHugh, E. M. Shevach, and R. N. Germain. 2002. Constitutive presentation of a natural tissue autoantigen exclusively by dendritic cells in the draining lymph node. *J. Exp. Med.* 196: 1079–1090.
30. Bliss, S. K., B. A. Butcher, and E. Y. Denkers. 2000. Rapid recruitment of neutrophils containing prestored IL-12 during microbial infection. *J. Immunol.* 165: 4515–4521.
31. Mason, N., J. Aliberti, J. C. Caamano, H. C. Liou, and C. A. Hunter. 2002. Cutting edge: identification of c-Rel-dependent and -independent pathways of IL-12 production during infectious and inflammatory stimuli. *J. Immunol.* 168: 2590–2594.
32. Rimoldi, M., M. Chieppa, V. Salucci, F. Avogadri, A. Sonzogni, G. M. Sampietro, A. Nespoli, G. Viale, P. Allavena, and M. Rescigno. 2005. Intestinal immune homeostasis is regulated by the crosstalk between epithelial cells and dendritic cells. *Nat. Immunol.* 6: 507–514.
33. Tanaka, J., K. Saga, M. Kido, H. Nishiura, T. Akamatsu, T. Chiba, and N. Watanabe. 2010. Proinflammatory Th2 cytokines induce production of thymic stromal lymphopoietin in human colonic epithelial cells. *Dig. Dis. Sci.* 55: 1896–1904.
34. Okazaki, T., Y. Otaka, J. Wang, H. Hiai, T. Takai, J. V. Ravetch, and T. Honjo. 2005. Hydronephrosis associated with antiurothelial and antinuclear autoantibodies in BALB/c-*Fcgr2b*$^{-/-}$*Pdcd1*$^{-/-}$ mice. *J. Exp. Med.* 202: 1643–1648.
35. Al-Shami, A., R. Spolski, J. Kelly, T. Fry, P. L. Schwartzberg, A. Pandey, C. L. Mackall, and W. J. Leonard. 2004. A role for thymic stromal lymphopoietin in CD4(+) T cell development. *J. Exp. Med.* 200: 159–168.

GASTROENTEROLOGY 2011;140:1322–1333

Dysregulated Generation of Follicular Helper T Cells in the Spleen Triggers Fatal Autoimmune Hepatitis in Mice

NOBUHIRO AOKI,[*,‡] MASAHIRO KIDO,[*,‡] SATORU IWAMOTO,[*,‡] HISAYO NISHIURA,[*,‡] RYUTARO MARUOKA,[*,‡] JUNYA TANAKA,[*,‡] TAKESHI WATANABE,[*] YOSHIMASA TANAKA,[*] TAKU OKAZAKI,[§] TSUTOMU CHIBA,[‡] and NORIHIKO WATANABE[*,‡]

Center for Innovation in Immunoregulative Technology and Therapeutics and ‡Department of Gastroenterology and Hepatology, Graduate School of Medicine, Kyoto University, Kyoto; and §Division of Immune Regulation, Institute for Genome Research, University of Tokushima, Tokushima, Japan

BACKGROUND & AIMS: To clarify mechanisms involved in the development of autoimmune hepatitis (AIH), we recently developed a mouse model of spontaneous AIH by inducing a concurrent loss of $Foxp3^+$ regulatory T cells and programmed cell death 1 (PD-1)–mediated signaling. Fatal AIH in these mice was characterized by severe T-cell infiltration and huge production of antinuclear antibodies (Abs). This study aims to identify induction sites, responsible T-cell subsets, and key molecules for induction of AIH. **METHODS:** To develop the mouse model of AIH, neonatal thymectomy (NTx) was performed on PD-1–deficient ($PD\text{-}1^{-/-}$) mice. We then conducted neonatal splenectomy or in vivo administration of Abs to cytokines, chemokines, or cell-surface molecules. **RESULTS:** In NTx-$PD\text{-}1^{-/-}$ mice, either neonatal splenectomy or in vivo $CD4^+$ T-cell depletion suppressed $CD4^+$ and $CD8^+$ T-cell infiltration in the liver. In the induction phase of AIH, splenic $CD4^+$ T cells were localized in B-cell follicles with huge germinal centers and showed the $Bcl6^+$ inducible costimulator $(ICOS)^+$ interleukin $(IL)\text{-}21^+$ IL-21 receptor $(IL\text{-}21R)^+$ follicular helper T (T_{FH}) cell phenotype. Blocking Abs to ICOS or IL-21 suppressed T_{FH}-cell generation and induction of AIH. In addition, IL-21 produced by T_{FH} cells drove $CD8^+$ T-cell activation. Splenic T_{FH} cells and $CD8^+$ T cells expressed CCR6, and CCL20 expression was elevated in the liver. Administration of anti-CCL20 suppressed migration of these T cells to the liver and induction of AIH. **CONCLUSIONS: Dysregulated T_{FH} cells in the spleen are responsible for the induction of fatal AIH, and CCR6-CCL20 axis-dependent migration of splenic T cells is crucial to induce AIH in NTx-$PD\text{-}1^{-/-}$ mice.**

Keywords: Autoimmune Liver Disease; Pathogenesis; Follicular Helper T Cells.

Human autoimmune hepatitis (AIH) shows varied clinical manifestations ranging from asymptomatic, mild chronic hepatitis to acute-onset fulminant hepatic failure. The histologic findings of AIH are characterized by a mononuclear cell infiltration invading the parenchyma, ranging from piecemeal necrosis to submassive lobular necrosis.[1,2] The serologic hallmark of AIH is the production of a variety of characteristic circulating autoantibodies (autoAbs), including anti-nuclear Abs (ANAs).[1,2] Although AIH appears to be a T cell-mediated autoimmune disease, it is unclear which type of effector T cells are involved and how the dysregulated T cells trigger the development of AIH.

Recently, we developed the first mouse model of spontaneous fatal AIH resembling acute-onset AIH presenting as fulminant hepatic failure in humans.[3] Neither programmed cell death 1 (PD-1)–deficient mice ($PD\text{-}1^{-/-}$ mice) nor BALB/c mice thymectomized 3 days after birth (NTx mice), which severely reduces the number of naturally arising $Foxp3^+$ regulatory T cells (Tregs) in periphery, developed inflammation of the liver. However, $PD\text{-}1^{-/-}$ BALB/c mice with neonatal thymectomy (NTx-$PD\text{-}1^{-/-}$ mice) developed fatal AIH, suggesting that immune dysregulation by a concurrent loss of naturally arising Tregs and PD-1–mediated signaling can induce fatal AIH. Because of the massive destruction of the parenchyma of the liver, these mice started to die as early as 2 weeks of age, with most dying by 4 weeks. In humans, liver tissue injury in AIH is mediated not only by $CD4^+$ but also by $CD8^+$ T cells.[4,5] Especially in acute-onset human AIH, activated $CD8^+$ T cells are thought to play a crucial role in the pathogenesis.[6] Fatal AIH in NTx-$PD\text{-}1^{-/-}$ mice was characterized by $CD4^+$ and $CD8^+$ T-cell infiltration with massive lobular necrosis and huge ANA production; activated $CD8^+$ T cells were mainly involved in progression to fatal hepatic damage.[3] We showed that the infiltrated $CD4^+$ and $CD8^+$ T cells in the severely damaged liver produced large amounts of inflammatory cytokines, such

Abbreviations used in this paper: AIH, autoimmune hepatitis; ANA, antinuclear antibody; APC, allo-phycocyanin; CXCR, CXC chemokine receptor; EAE, experimental autoimmune encephalomyelitis; GC, germinal center; ICOS, inducible costimulator; IFN, interferon; Ig, immunoglobulin; IL, interleukin; IL-21R, IL-21 receptor; NTx, neonatal thymectomy; NTx-$PD\text{-}1^{-/-}$ mice, PD-1–deficient BALB/c mice thymectomized 3 days after birth; PD-1, programmed cell death 1; PD-L, programmed cell death ligand; PNA, peanut agglutinin; RAG2, recombination activating gene 2; T_{FH}, follicular helper T; Th, T helper; Tregs, regulatory T cells.

0016-5085/$36.00
doi:10.1053/j.gastro.2011.01.002

as interferon (IFN)-γ and tumor necrosis factor-α. However, it is unclear whether these effector T cells are also crucial in the induction phase of the disease.

Follicular helper T (T_{FH}) cells are a newly defined effector T cell subset that provides powerful help to B cells in forming germinal centers (GCs).[7-9] T_{FH} cells arise from activated T cells that express Bcl6, a master transcription factor for T_{FH}-cell differentiation.[8,9] Differentiated T_{FH} cells express interleukin (IL)-21, IL-21 receptor (IL-21R), inducible costimulator (ICOS), CXC chemokine receptor (CXCR)5, and PD-1. IL-21 and ICOS are indispensable for T_{FH}-cell generation and helper function to B cells.[7-9] CXCR5 promotes the colocalization of T_{FH} cells and B cells in GCs.[7-9] Although $CXCR5^+$ T_{FH} cells are localized mainly in the GC^+ B-cell follicles, a recent study showed that circulating T cells resembling T_{FH} cells existed in the peripheral blood of patients with B cell–mediated autoimmunity.[10] In addition, IL-21 has the potential to modulate the activity of $CD8^+$ T cells and other immune and nonimmune cells in vivo.[11] Although AIH appears to be a T cell–mediated autoimmune disease, it is characterized by hyper-γ-globulinemia and the production of a variety of circulating autoAbs, suggesting that B-cell activation including B cell–mediated autoimmunity is associated with its development. Thus, it may be possible that dysregulated T_{FH} cells are involved in both T cell- and B cell–mediated autoimmunity in AIH.

In this study, using our new mouse model of AIH, we examined the T-cell subsets responsible for induction of AIH and the mechanisms by which these T cells initiate fatal AIH. We found that splenic $CD4^+$ T cells are responsible for induction of fatal AIH. In these mice, splenic $CD4^+$ T cells were autonomously differentiated into T_{FH} cells. Moreover, dysregulated T_{FH} cells not only promoted ANA production but also directly migrated into the liver, triggering the induction of fatal AIH.

Materials and Methods

Methods

All protocols for mice, enzyme-linked immunosorbent assay, administration of Abs in vivo, histologic and immunohistologic analysis, flow cytometry analysis and isolation of lymphocytes, adoptive transfer, real-time quantitative reverse-transcription polymerase chain reaction, and T-cell coculture are detailed in Supplementary Methods.

Statistical Analysis

The data are presented as the mean values ± standard deviations. Statistical analysis was performed by the Student *t* test for pairwise comparisons. Survival rates were estimated by the Kaplan–Meier method and compared with the log-rank test. *P* values below .05 were considered significant.

Results

Splenic $CD4^+$ T Cells Are Responsible for Induction of Fatal AIH

Fatal AIH developed in 3-week-old NTx-PD-$1^{-/-}$ mice was characterized by severe $CD4^+$ and $CD8^+$ T-cell infiltration.[3] To examine whether $CD4^+$ and/or $CD8^+$ T cells are indispensable for the development of fatal AIH, NTx-PD-$1^{-/-}$ mice were injected intraperitoneally at 1 day after NTx and then once a week with either anti-CD4 or anti-CD8 monoclonal antibodies (mAbs). After 4 injections of anti-CD4 or anti-CD8, the number of $CD4^+$ or $CD8^+$ T cells in the periphery was greatly reduced, respectively, and fatal AIH was suppressed (Figure 1*A* and data not shown). Importantly, depletion of $CD4^+$ T cells inhibited the infiltration of $CD8^+$ T cells in the liver, whereas depletion of $CD8^+$ T cells allowed $CD4^+$ T cells to infiltrate (Figure 1*B*). These data suggest that both $CD4^+$ and $CD8^+$ T cells are indispensable for the development of fatal AIH and that the infiltration of $CD8^+$ T cells in the liver is regulated by $CD4^+$ T cells.

Three-week-old NTx-PD-$1^{-/-}$ mice with severe AIH showed splenomegaly, and the spleen in these mice became enlarged as early as 2 weeks of age (Figure 1C). To determine whether the spleen is an induction site for fatal AIH, we performed neonatal splenectomy in these mice. We found that neonatal splenectomy suppressed mononuclear infiltration as well as destruction of organ structure in the liver, leading to a significantly higher survival rate (Figure 1*D* and *E*). We had previously demonstrated that transfer of total but not $CD4^+$ T-cell depleted splenocytes from NTx-PD-$1^{-/-}$ mice into recombination activating gene 2 $(RAG2)^{-/-}$ mice induced the development of severe hepatitis.[3] Taken together, these data suggest that the spleen is an induction site for AIH and that splenic $CD4^+$ T cells are responsible for induction of fatal AIH.

Splenic $CD4^+$ T Cells in NTx-PD-$1^{-/-}$ Mice Are Preferentially Localized Within GC-Bearing B-Cell Follicles

After the spleen became enlarged at 2 weeks of age, hepatic damage from AIH was apparent at 2 to 3 weeks in NTx-PD-$1^{-/-}$ mice.[3] When we looked in situ at the spleen of 2-week-old NTx-PD-$1^{-/-}$ mice, most of the $CD4^+$ T cells were preferentially localized within $B220^+$ B-cell follicles, whereas $CD8^+$ T cells were mainly localized outside the follicles. Interestingly, B-cell follicles with $CD4^+$ T-cell accumulation autonomously developed peanut agglutinin $(PNA)^+$ GCs (Figure 1*F*, *left lower panels*, and Supplementary Figure 1). Seven days after thymectomy, 1.5-week-old NTx-PD-$1^{-/-}$ mice showed scattered accumulation of $CD4^+$ T cells with $B220^+$ B cells in the spleen (Figure 2*A*). Diffuse accumulation of $CD4^+$ T cells in the follicles with GC formation developed in the spleen of 2-week-old mice and progressed in

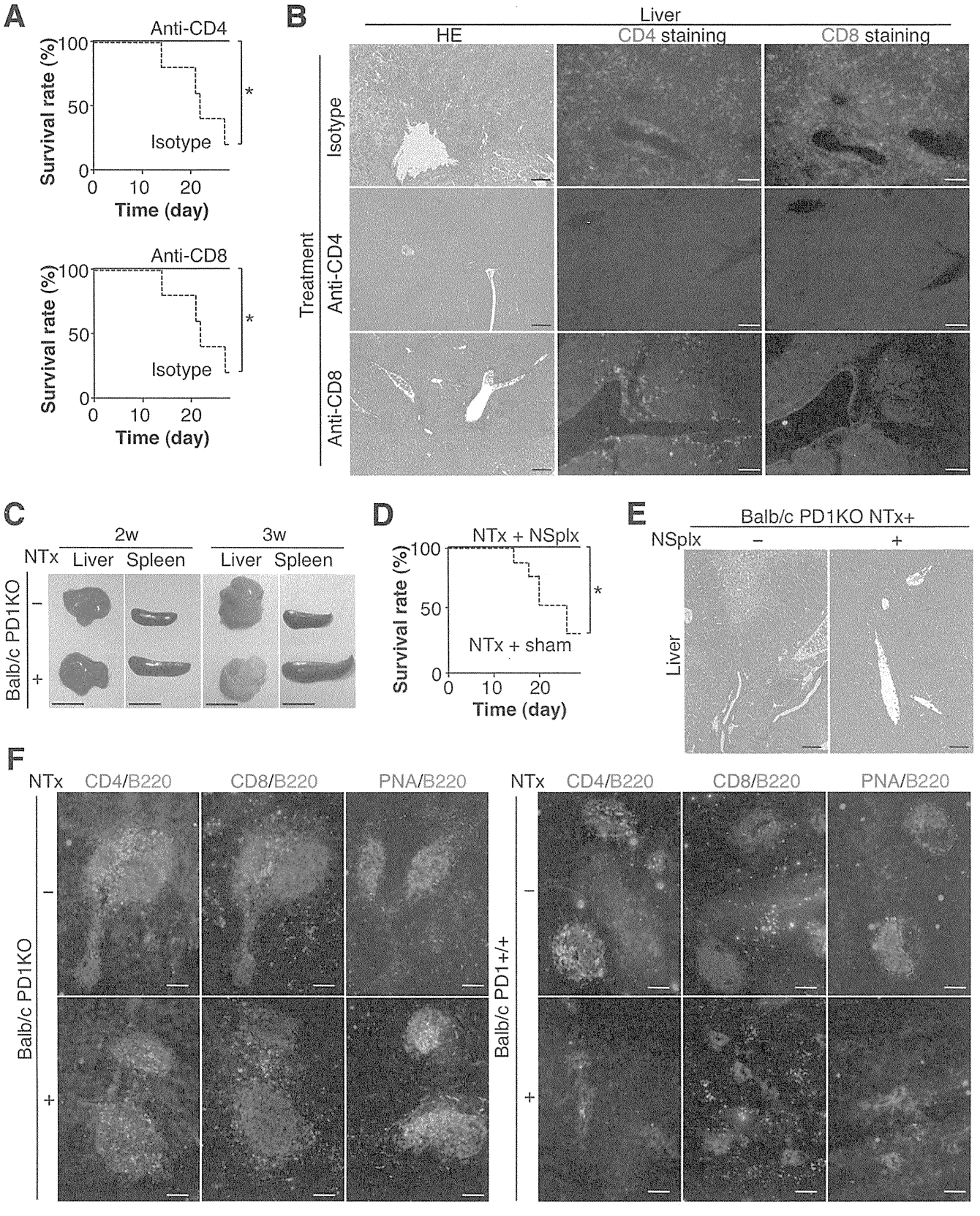
A
Anti-CD4
Survival rate (%)
100
50
0
Isotype
*
0 10 20
Time (day)
Anti-CD8
Survival rate (%)
100
50
0
Isotype
*
0 10 20
Time (day)
B
Liver
HE
CD4 staining
CD8 staining
Treatment
Isotype
Anti-CD4
Anti-CD8
C
2w
3w
NTx
Liver Spleen
Liver Spleen
Balb/c PD1KO
–
+
D
NTx + NSplx
Survival rate (%)
100
50
0
NTx + sham
*
0 10 20
Time (day)
E
Balb/c PD1KO NTx+
NSplx
–
+
Liver
F
NTx
CD4/B220
CD8/B220
PNA/B220
Balb/c PD1KO
–
+
NTx
CD4/B220
CD8/B220
PNA/B220
Balb/c PD1+/+
–
+

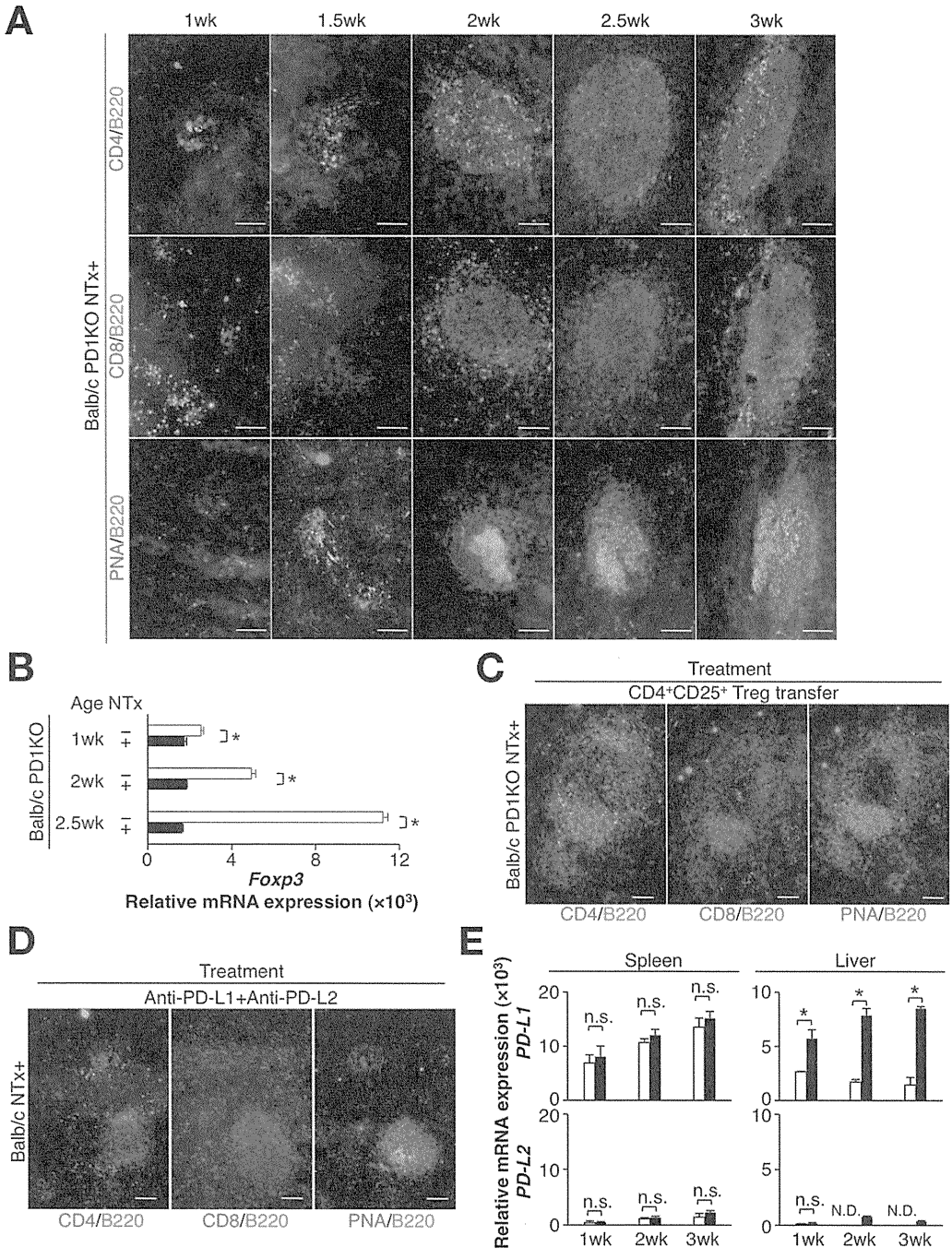

Figure 2. Autonomous localization of splenic CD4$^+$ T cells within GC$^+$ follicles depends on concurrent loss of naturally arising Tregs and PD-1 mediated signaling. (*A*) The spleens from indicated mice at 1 to 3 weeks of age were stained as described in Figure 1*F*. (*B*) Foxp3 mRNA expression by CD4$^+$ T cells from the spleen of indicated mice. (*C*) Double immunostainings of the spleen from 2-week-old NTx-PD-1$^{-/-}$ mice transferred with splenic Tregs from normal BALB/c mice. The spleens were stained as described in Figure 1*F*. (*D*) Double immunostainings of the spleen in 2-week-old NTx mice injected at days 3 and 10 with anti-PD-L1 and anti-PD-L2. The spleens were stained as described in Figure 1*F*. (*E*) PD-L1 and PD-L2 mRNA expressions of liver and spleen of PD-1$^{-/-}$ mice at indicated age in weeks with (*solid columns*) or without (*open columns*) NTx. *Bars* indicate the mean of each group, and *short bars* indicate the standard deviation. *$P < .05$. N.D., not detected; n.s., not significant. All *scale bars*, 100 μm.

Figure 1. Splenic CD4$^+$ T cells are responsible for induction of fatal AIH. (*A* and *B*) NTx-PD-1$^{-/-}$ mice were injected intraperitoneally at 1 day after NTx and then once a week with anti-CD4 (n = 5), anti-CD8 (n = 5), or isotype (n = 5) Abs. After 4 injections, mice at 4 weeks of age were killed, and the livers were harvested. (*A*) Survival rate of the mice and (*B*) stainings of the liver for hematoxylin and eosin (*HE*), CD4, and CD8 at 4 weeks. (*C*) Macroscopic view of the liver and spleen from indicated mice. (*D*) Survival rate and (*E*) histology of the liver from 4-week-old NTx-PD-1$^{-/-}$ mice with (n = 7) or without (n = 9) neonatal splenectomy (*NSplx*). (*F*) The spleens from indicated mice at 2 weeks of age were stained with FITC-conjugated anti-CD4, anti-CD8, or PNA (*green*) and biotin-labeled anti-B220 followed by Texas red-conjugated avidin (*red*). *Scale bars*, 1 cm in *C* and 100 μm in others. *$P < .05$.

2.5-week-old mice. Although GC size was slightly increased in the spleen of 3-week-old NTx-PD-1$^{-/-}$ mice, localization of CD4$^+$ T cells moved into the marginal region of follicles (Figure 2*A*, *right panels*).

The rapid accumulation of CD4$^+$ T cells in the follicles with GC formation depended on concurrent loss of naturally arising Tregs and PD-1–mediated signaling because neither PD-1$^{-/-}$ mice nor NTx mice at 2 weeks of age showed any of these phenotypes (Figure 1*F*) nor did they develop fatal AIH.[3] In addition, Foxp3 expression of splenic CD4$^+$ T cells of NTx-PD-1$^{-/-}$ mice was severely reduced (Figure 2*B*), and transfer of Tregs from either normal BALB/c or PD-1$^{-/-}$ mice into NTx-PD-1$^{-/-}$ mice suppressed GC formations in the spleen (Figure 2*C* and data not shown). On the other hand, concomitant administration of blocking mAbs to programmed cell dealth 1 ligand (PD-L)1 and PD-L2 induced an accumulation of CD4$^+$ T cells in the follicles and development of GCs in the spleen of NTx mice at 2 weeks (Figure 2*D*). Interestingly, we found that, in one of the PD-1 ligands, PD-L1 messenger RNA (mRNA) expression was up-regulated in the liver of 1- to 3-week-old NTx-PD-1$^{-/-}$ mice (Figure 2*E*).

Splenic CD4$^+$ T Cells in NTx-PD-1$^{-/-}$ Mice Display the Molecular Signature of T_{FH} Cells and Directly Induce AIH

We next examined whether accumulated CD4$^+$ T cells in the follicles of the spleen display the molecular signature of T_{FH} cells. CD4$^+$ T cells in the spleen of 1-week-old NTx-PD-1$^{-/-}$ mice showed increased IL-21 mRNA expression (Figure 3*A*). In addition, CD4$^+$ T cells isolated from the spleen of 2- to 3-week-old NTx-PD-1$^{-/-}$ mice also showed increased Bcl-6 and IL-21 mRNA expressions (Figure 3*B*). Protein expressions of Bcl-6, IL-21, ICOS, and CXCR5 were detectable in these cells (Figure 3*C* and *D*, *upper panels*), indicating some key features of T_{FH} cells.[7–9] In addition, B220$^+$ B cells expressed FAS and GL7 (Figure 3*D*, *lower panels*), hallmarks of GC B cells.[7–9] Moreover, GC size increased in the spleen of mice aged 1 to 3 weeks (Supplementary Figure 2). Three-week-old NTx-PD-1$^{-/-}$ mice showed hyper-γ-globulinemia and vast production of class-switched ANAs (Supplementary Figure 3).

To investigate whether splenic T_{FH} cells directly trigger the development of T cell–mediated AIH, we purified ICOS$^+$CD4$^+$ T_{FH} cells or ICOS$^-$CD4$^+$ T cells from the spleen of 2.5-week-old NTx-PD-1$^{-/-}$ mice and transferred those T cells into T- and B cell–deficient RAG2$^{-/-}$ mice. In contrast to transfer of ICOS$^-$CD4$^+$ T cells, transfer of ICOS$^+$CD4$^+$ T_{FH} cells induced mononuclear cell infiltrations in the portal area of the liver and significantly increased serum levels of aspartate aminotransferase and alanine aminotransferase in recipient mice at 3 weeks after transfer (Figure 3*E* and *F*). These data suggest that splenic T_{FH} cells in NTx-PD-1$^{-/-}$ mice can directly trigger T cell–mediated AIH.

Key Features of T_{FH} Cells, Expressions of IL-21 and Bcl6 Are Sustained in Splenic and Hepatic CD4$^+$ T Cells in the Development of AIH

To further characterize CD4$^+$ T cell subsets in the development of AIH, we isolated splenic and hepatic CD4$^+$ T cells from NTx-PD-1$^{-/-}$ mice aged 1 to 3 weeks and measured expression levels of mRNA encoding master regulators and related cytokines for different T-cell subsets. Although not only T_{FH} cells but also T helper (Th) 17 cells are reported to express IL-21,[12] isolated CD4$^+$ T cells from the spleen and liver showed up-regulated IL-21 but not IL-17A mRNA expression in NTx-PD-1$^{-/-}$ mice (Figure 4*A*), suggesting that these CD4$^+$ T cells are not likely to be a Th17 subset. When we looked at master regulators for T-cell subsets, in NTx-PD-1$^{-/-}$ mice at 1 week, splenic CD4$^+$ T cells significantly up-regulated mRNA expression of Bcl-6 but not RORγT, GATA-3, or T-bet (Figure 4*B*). In addition, in the induction phase of AIH in NTx-PD-1$^{-/-}$ mice at 2 weeks, not only splenic CD4$^+$ T cells but also hepatic CD4$^+$ T cells significantly up-regulated mRNA expression of Bcl-6 but not others. Notably, although T-bet expression was also significantly up-regulated in both splenic and hepatic CD4$^+$ T cells in the progression phase of AIH in NTx-PD-1$^{-/-}$ mice at 3 weeks, up-regulated expression of Bcl-6 was sustained in those CD4$^+$ T cells.

Administration of Either Anti-ICOS or Anti–IL-21 Completely Suppresses Not Only T_{FH}-cell Generation but Also Induction of Fatal AIH

IL-12 is decisive in the development of Th1 subsets, whereas ICOS and IL-21 are indispensable for T_{FH}-cell differentiation and maturation.[7–9] To examine further whether differentiation of Th1 and/or T_{FH} subsets is critical in the induction of AIH, we administered blocking mAbs to IL-12p40, ICOS, or IL-21. Although production of ANA in both immunoglobulin (Ig)G1 and IgG2a subclasses increased in NTx-PD-1$^{-/-}$ mice (Supplementary Figure 3), injections of anti–IL-12p40 induced reciprocal alteration of ANA in Th1-dependent IgG2a and Th2-dependent IgG1 subclasses (Supplementary Figure 4). However, the neutralization of IL-12 did not significantly reduce the size of GCs in the spleen at 4 weeks (Figure 4*C*). In contrast, after 4 injections of either anti-ICOS or anti–IL-21, NTx-PD-1$^{-/-}$ mice at 4 weeks showed markedly suppressed GC formation in the spleen and accumulation of CD4$^+$ T cells in the follicles (Figures 4*C* and *D* and Supplementary Figures 5*A* and 6*A*). In addition, hyper-γ-globulinemia and ANA production, including class-switched Abs, were greatly reduced in those mice (Supplementary Figure 5*C*, and data not shown). Importantly, although neutralizing IL-12 did not suppress AIH development, either anti-ICOS or anti–IL-21 injections completely suppressed infiltration of not only

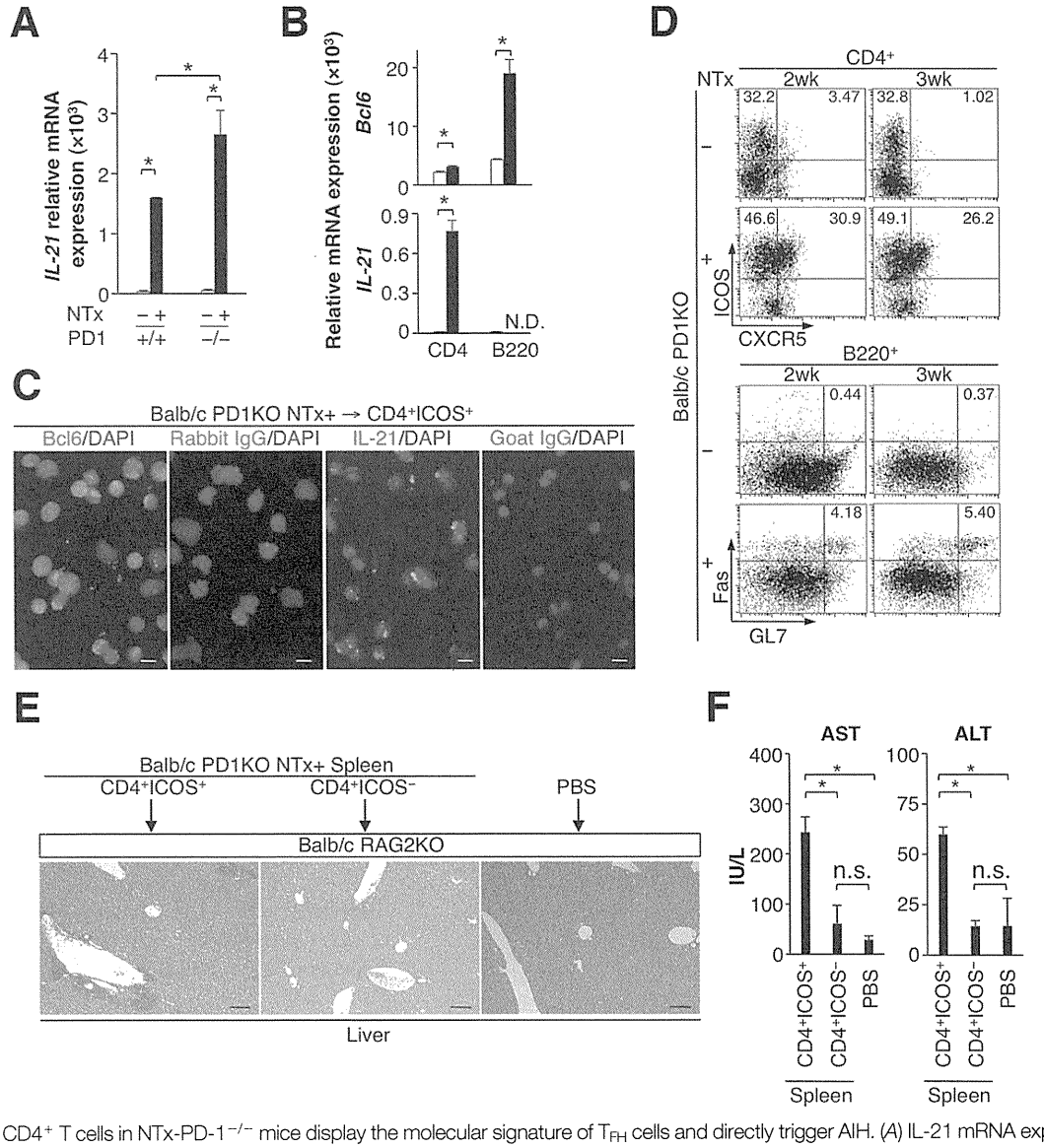

Figure 3. Splenic CD4$^+$ T cells in NTx-PD-1$^{-/-}$ mice display the molecular signature of T_{FH} cells and directly trigger AIH. (*A*) IL-21 mRNA expressions by isolated splenic CD4$^+$ T cells in indicated mice at 1 week of age. (*B*) Bcl6 and IL-21 mRNA expressions by isolated splenic CD4$^+$ T cells and B220$^+$ B cells in 2.5-week-old PD-1$^{-/-}$ mice with (*solid columns*) or without (*open columns*) NTx. (*C*) Double immunostainings of isolated splenic CD4$^+$ICOS$^+$ T cells from 2.5-week-old NTx-PD-1$^{-/-}$ mice with DAPI and anti-Bcl6, anti—IL-21, or the isotype controls. (*D*) Flow cytometric analysis of CD4$^+$ T cells (*upper panels*) and B220$^+$ cells (*lower panels*) in indicated mice at 2 or 3 weeks of age. The cells were stained with indicated Abs as described in the Materials and Methods section. Numbers in *plots* indicate percent cells in each gate. (*E and F*) CD4$^+$ICOS$^+$ T cells or CD4$^+$ICOS$^-$ T cells from the spleen of 2.5-week-old NTx-PD-1$^{-/-}$ mice were transferred into RAG2$^{-/-}$ mice intravenously. (*E*) Staining of the liver for H&E 3 weeks after transfer. (*F*) Serum levels of the liver transaminase, aspartate aminotransferase (AST), and alanine aminotransferase (ALT). *Bars* indicate the mean of each group, and *horizontal short bars* indicate the standard deviation. *$P < .05$. N.D., not detected; n.s., not significant. *Scale bars*, 10 μm in *C* and 100 μm in others.

CD4$^+$ T cells but also CD8$^+$ T cells in the liver as well as liver destruction, resulting in a significantly higher survival rate (Figure 4*D–F* and Supplementary Figures 5*B* and 6*B*). These data suggest a link between generation of T_{FH} cells and induction of AIH.

IL-21 Is a Key Cytokine for Not Only T_{FH} Generation but Also Activation of CD8$^+$ T Cells

Next, we examined how CD4$^+$ T cells help CD8$^+$ T cells in developing AIH. In the induction phase in 2-week-old mice, CD8$^+$ T cells not only in the liver but also in the spleen showed Ki-67^{high} activated T-cell phenotype with highly proliferating potential (Figure 5*A*). IL-21 potentially modulates activity of CD8$^+$ T cells,[11] and T_{FH} cells in the spleen produced IL-21 (Figures 3*A–C* and 4*A*). Moreover, IL-21R mRNA expression in splenic CD8$^+$ T cells was elevated in NTx-PD-1$^{-/-}$ mice (Figure 5*B*). Therefore, to examine whether CD4$^+$ T-cell help for CD8$^+$ T-cell activation in the spleen depends on IL-21 in the induction phase of AIH, CD8$^+$ T cells were purified from the spleen of PD-1$^{-/-}$ mice. These CD8$^+$ T cells were cultured with CD4$^+$ T cells from the spleen of

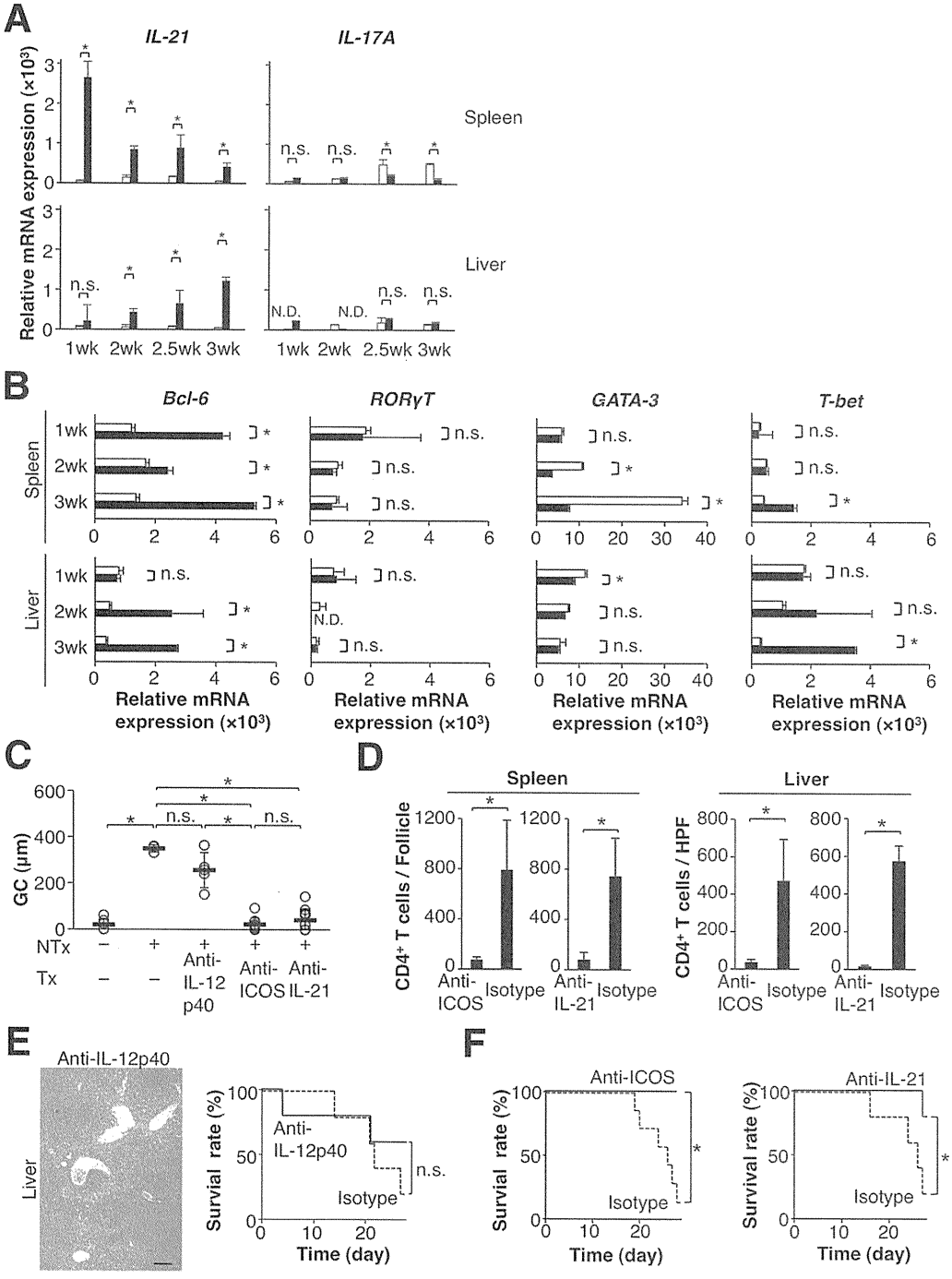

Figure 4. T_{FH}-cell generation rather than Th1 differentiation is primarily involved in the induction of fatal AIH. (*A* and *B*) Splenic and hepatic CD4$^+$ T cells were isolated from indicated aged PD-1$^{-/-}$ mice with (*solid columns*) or without (*open columns*) NTx. Real-time quantitative RT-PCR analysis was performed to measure the expression levels of mRNA encoding indicated master regulators for T-cell subsets and related cytokines. (*C–F*) NTx-PD-1$^{-/-}$ mice were intraperitoneally injected as described in Figure 1*B* with anti–IL-12p40, anti-ICOS, or anti–IL-21 Abs. After 4 injections, mice at 4 weeks of age were killed, and the spleens and livers were harvested. In *panel C*, the size of GCs in the spleen of indicated mice is shown. Spleens were stained as in Figure 1*F*. (*C*) Each *open circle* represents a size of GC measured in high-power fields. (*D*) CD4$^+$ T-cell numbers in the follicles of the spleen (*left*) or the liver (*right*) of indicated mice. (*E*) H&E staining of the liver and survival rate in NTx-PD-1$^{-/-}$ mice injected with anti–IL-12p40 (n = 5) or isotype (n = 5) Abs. (*F*) Survival rate in NTx-PD-1$^{-/-}$ mice with anti-ICOS (n = 5) or isotype (n = 7) Abs and those with anti–IL-21 (n = 5) or isotype (n = 5) Abs. *Bars* indicate the mean of each group, and *short bars* indicate the standard deviation. *$P < .05$. N.D., not detected; n.s., not significant. All *scale bars*, 100 μm.

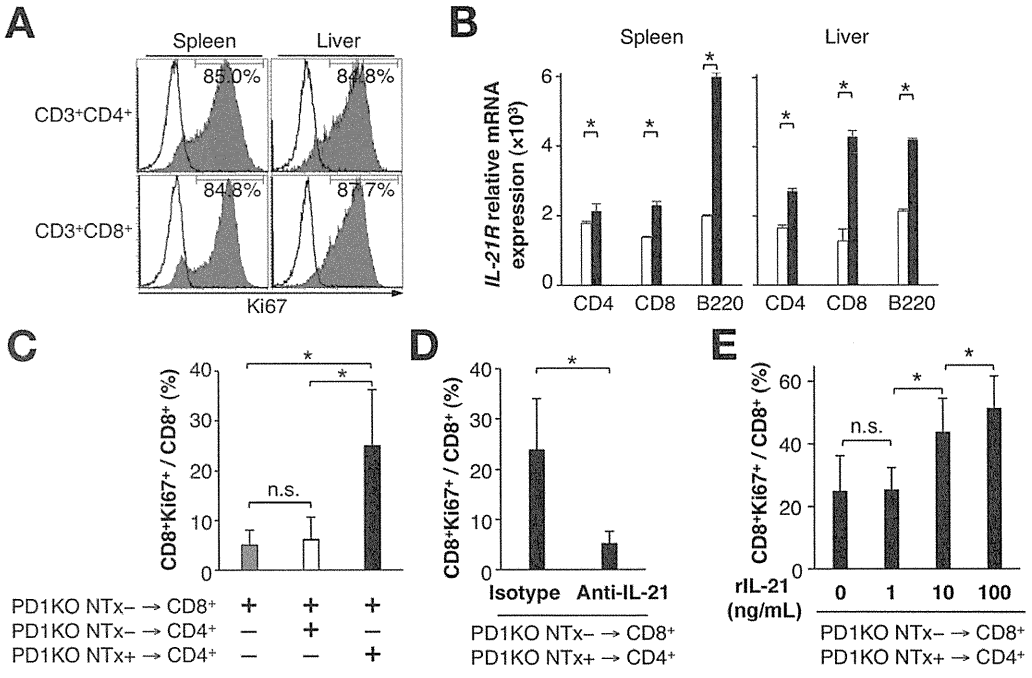

Figure 5. IL-21 is a key cytokine for $CD8^+$ T-cell activation induced by $CD4^+$ T cells. (*A*) Flow cytometric analysis of cells in the spleen and liver of 2-week-old NTx-PD-$1^{-/-}$ mice. Phenotypes of $CD3^+CD4^+$ and $CD3^+CD8^+$ T cells were shown. *Solid histograms* represent anti–Ki-67 staining; *open histograms* represent the isotype controls. *Numbers* indicate percent of $Ki67^+$ cells. Data represent 1 of 3 separate experiments. (*B*) IL-21R mRNA expressions by isolated $CD4^+$, $CD8^+$ T cells, and $B220^+$ B cells of the spleen and liver in 2.5-week-old PD-$1^{-/-}$ mice with (*solid columns*) or without (*open columns*) NTx. *Bars* indicate the mean of each group, and *horizontal short bars* indicate the standard deviation. (*C–E*) Flow cytometric analysis of $CD8^+$ T cells. $CD8^+$ T cells were purified from the spleen of PD-$1^{-/-}$ mice and then cultured with $CD4^+$ T cells from the spleen of 2-week-old PD-$1^{-/-}$ mice with or without NTx. After 1 day of culture with indicated conditions, percent of $Ki67^+$ cells in $CD8^+$ T-cell population was determined by flow cytometry. *Bars* indicate the mean of triplicated wells of each group, and *horizontal short bars* indicate the standard deviation. $^*P < .05$. n.s., not significant.

2-week-old PD-$1^{-/-}$ mice with or without NTx. After 1 day of culture, $CD8^+$ T cells cultured with $CD4^+$ T cells from NTx-PD-$1^{-/-}$ mice showed a significant increase of $Ki67^+$ cells in the $CD8^+$ T-cell population, indicating that activated $CD4^+$ T cells in the spleen of NTx-PD-$1^{-/-}$ mice have the potential to induce $CD8^+$ T-cell activation (Figure 5*C*). In addition, neutralizing antibodies to IL-21 suppressed increase of $Ki67^+$ cells in $CD8^+$ T-cell population cultured with those $CD4^+$ T cells, suggesting that IL-21 produced by T_{FH} cells drives activation of $CD8^+$ T cells (Figure 5*D*). Moreover, recombinant IL-21 further increased $Ki67^+CD8^+$ T cells cultured with those $CD4^+$ T cells dose dependently (Figure 5*E*). These data suggest that IL-21 is a key cytokine for not only T_{FH} generation but also activation of $CD8^+$ T cells in AIH development.

The CCR6-CCL20 Axis Is Crucial for Splenic T-Cell Migration Into the Liver, Inducing Fatal AIH

Finally, to examine how dysregulated T_{FH} cells and activated $CD8^+$ T cells migrate from the spleen into the liver in the induction phase of AIH, we analyzed chemokine receptor expression of T cells in the spleen and liver by flow cytometry. Previously, we showed that $CD4^+$ T cells in the spleen and liver expressed chemokine receptor CCR6 in NTx-PD-$1^{-/-}$ mice.[3] In $CD4^+$ T cells of 2-week-old NTx-PD-$1^{-/-}$ mice, $CCR6^+$ and, to a lesser extent, $CCR9^+$ cells increased (Figure 6*A*). The predominant increase of $CCR6^+$ cells was observed only at 2 weeks in the spleen and liver but not in mesenteric lymph nodes. In contrast, in 3-week-old mice, $CXCR3^+$ cells were predominant in splenic and hepatic $CD4^+$ T cells compared with $CCR6^+$ or $CCR9^+$ cells (Figure 6*B*). Splenic $CCR6^+CD4^+$ T cells in NTx-PD-$1^{-/-}$ mice contained $CXCR5^+CCR6^+$ population (Figure 6*C*, *left panels*), suggesting that these T cells retained the molecular signature of T_{FH} cells. In 3-week-old mice, $CXCR5^+$ $CCR6^-$ population was further increased, whereas the $CXCR5^{+or-}CCR6^+$ population was decreased (Figure 6*C*, *right panels*), suggesting preferential loss of $CCR6^+$ cells from the spleen after induction of AIH. In addition to $CD4^+$ T cells, in $CD8^+$ T cells, predominant increases of $CCR6^+$ cells in the spleen and liver were also found in the induction phase of AIH (Figure 6*D* and *E*). Moreover, gene expression of CCR6 ligand CCL20, but not CCR9 ligand CCL25, was elevated in the liver of 1.5- and 2-week-old NTx-PD-$1^{-/-}$ mice (Figure 6*F*). These data suggest that CCR6-expressing T cells in the spleen may migrate into CCL20-expressing liver and trigger the development of fatal AIH.

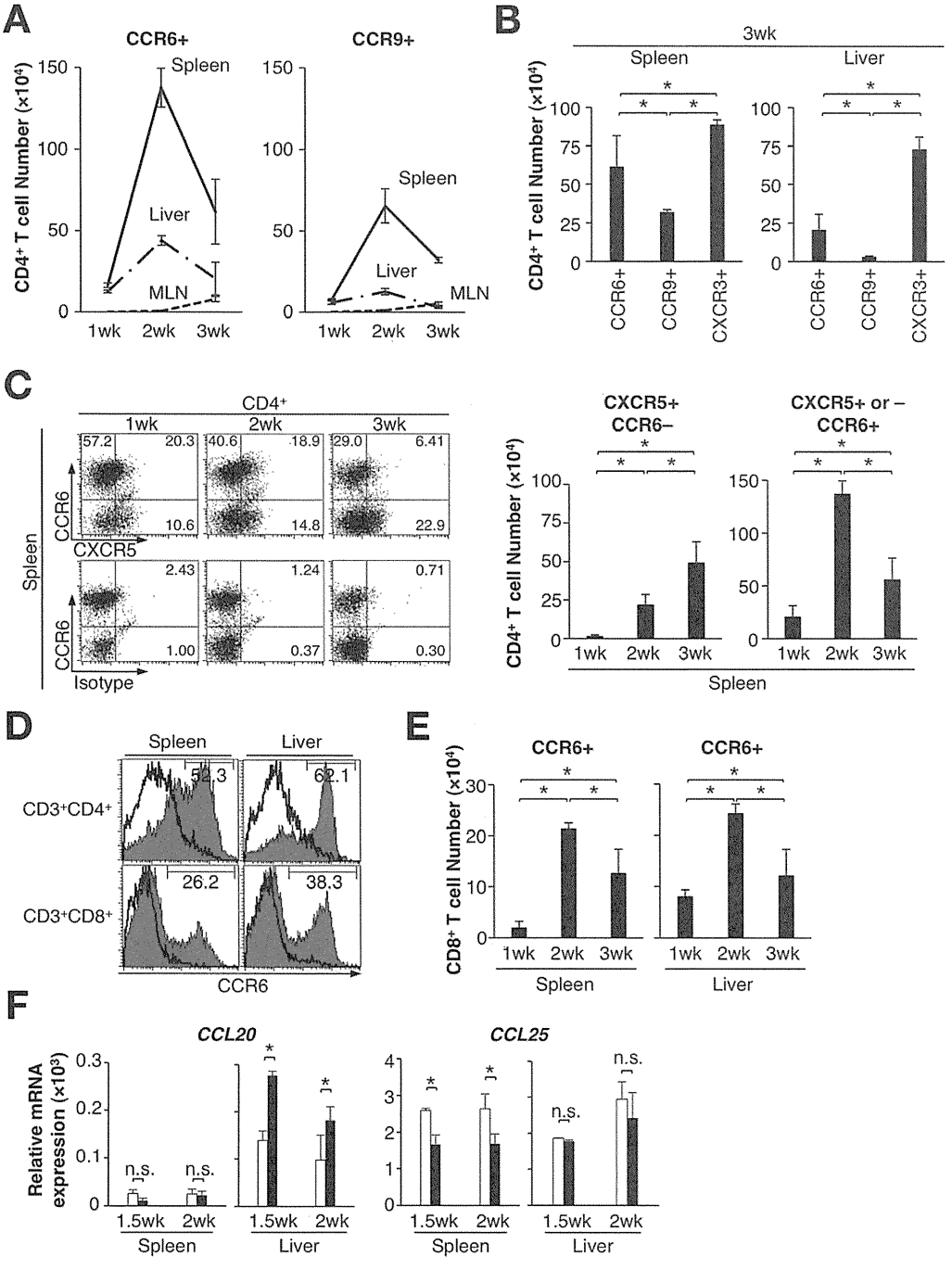

Figure 6. CCR6$^+$ cells are predominantly increased in CD4$^+$ and CD8$^+$ T cells in the spleen and liver only in the induction phase of AIH. (*A–E*) Cells in the spleen, liver, and mesenteric lymph nodes (*MLN*) of NTx-PD-1$^{-/-}$ mice at the indicated age were stained with FITC-anti-CD3e, APC-Cy7-anti-CD4 and PE-anti-CCR6, -anti-CCR9, or -anti-CXCR3 (*A*, *B*, and *D*, *upper panels*), with FITC-anti-CXCR5, PE-anti-CCR6, and APC-Cy7-anti-CD4 (*C*), or with FITC-anti-CD3e, PE-anti-CCR6 APC-anti-CD8 (*D*, *lower panels*, and *E*). Flow cytometric analyses were assessed as in Figure 3*D*. Numbers of indicated T-cell populations were calculated by (percentage of the cells in viable cells) × (number of viable cells) (*A*, *B*, *C*, *right panels*, and *E*). *Numbers* indicate percent of indicated gates (*C*, *left panels*; *D*). (*F*) CCL20 or CCL25 mRNA expressions in the spleen and liver of PD-1$^{-/-}$ mice at indicated age with (*solid columns*) or without (*open columns*) NTx. *Bars* indicate the mean of each group, and *horizontal short bars* indicate the standard deviation. *$P < .05$. n.s., not significant.

To determine whether the CCR6-CCL20 axis is critical for migration of splenic T cells into the liver and triggering fatal AIH, we administered mAbs blocking to CCL20. After 3 injections of anti-CCL20 Abs, the spleen of 3-week-old NTx-PD-1$^{-/-}$ mice showed further accumulation of T_{FH} cells in the GC$^+$ follicles diffusely (Figure 7*A* and *B*, *left panel*). These findings contrasted with the spleens of non-injected 3-week-old NTx-PD-1$^{-/-}$ mice, in which splenic

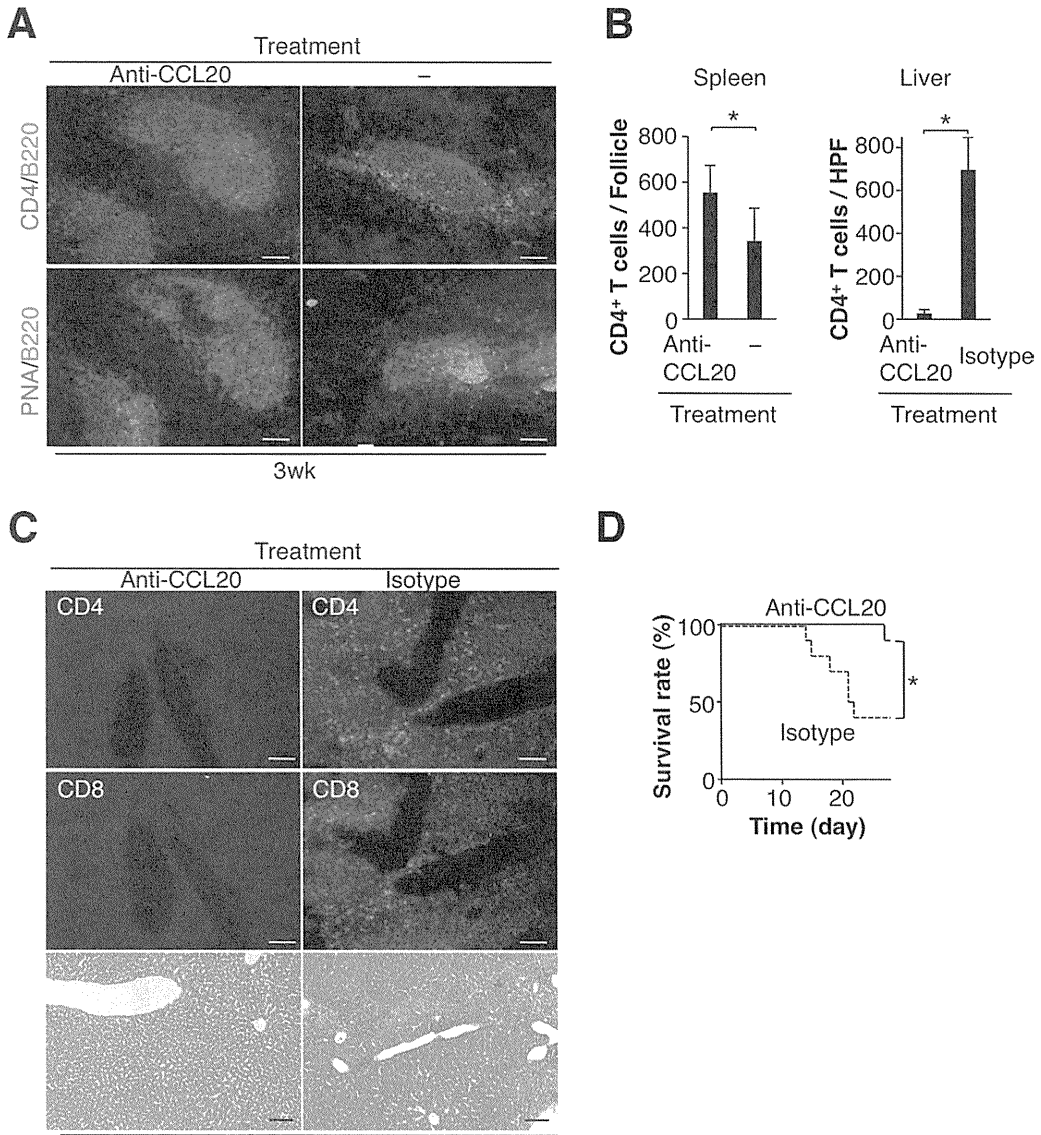

Figure 7. The CCR6-CCL20 axis plays a crucial role for both migration of splenic T_{FH} cells into the liver and induction of fatal AIH. (*A–D*) NTx-PD-1$^{-/-}$ mice were injected intraperitoneally as described in Figure 1 with anti-CCL20 (n = 10) or isotype (n = 10) Abs. The spleen and liver were stained as in Figure 1*B* and 1*F*. (*A*) Double immunostainings of the spleen of 3-week-old mice. (*B*) CD4$^+$ T-cell numbers in the follicles of the spleen of 3-week-old (*left*) and in the liver of 4-week-old (*right*) of indicated mice. (*C*) Immunostainings for CD4 and CD8 and H&E staining (*lower panels*) of the liver of 4-week-old mice. (*D*) Survival rate of each group of 4-week-old mice. *Bars* indicate the mean of each group, and *horizontal short bars* indicate the standard deviation. *$P < .05$. All *scale bars*, 100 μm.

T_{FH} cells were mainly localized in the marginal region of follicles (Figure 7*A*), and with the spleens from anti-ICOS or anti–IL-21 injected mice, in which splenic CD4$^+$ T cells were greatly reduced (Figure 4*D*). Importantly, administering anti-CCL20 suppressed infiltration of CD4$^+$ and CD8$^+$ T cells into the liver and liver destruction, with a significantly increased survival rate at 4 weeks (Figure 7*B*, *right panel*, 7*C* and *D*). These data suggest that, in the induction phase of AIH, the CCR6-CCL20 axis is crucial for migration of dysregulated T_{FH} cells and activated CD8$^+$ T cells from the spleen into the liver.

Discussion

We demonstrated herein that in our mouse model of spontaneous AIH induced by a concurrent loss of Tregs and PD-1–mediated signaling, splenic CD4$^+$ T cells are crucial in the development of fatal AIH. In the induction phase, splenic CD4$^+$ T cells in these mice showed the T_{FH}-cell phenotype, and CCR6-expressing T_{FH} cells and activated CD8$^+$ T cells in the spleen preferentially recruited to the liver via CCL20, triggering the induction of fatal AIH.

We found that $CD4^+$ T cells in the induction site of AIH, the spleen, were exclusively localized in GC-bearing B-cell follicles. In the induction phase of AIH, these $CD4^+$ T cells up-regulated expression of Bcl6, the master transcription factor for T_{FH}-cell differentiation, and showed the $IL\text{-}21^+IL\text{-}21R^+ICOS^+CXCR5^+$ T_{FH}-cell phenotype.[7-9] In addition, B cells in the spleen contained FAS^+GL7^+ GC B cells, and hyper-γ-globulinemia, and huge production of class-switched ANAs were observed in the serum from NTx-PD-$1^{-/-}$ mice. Moreover, in vivo administration of blocking Abs to ICOS or IL-21, indispensable for T_{FH}-cell generation and maturation,[7-9] inhibited accumulation of $CD4^+$ T cells in B-cell follicles and GC formation in the spleen, and suppressed hyper-γ-globulinemia, class-switched ANA production as well as induction of AIH. Importantly, adaptive transfer of the splenic T_{FH} cells from NTx-PD-$1^{-/-}$ mice directly triggered T cell–mediated AIH. From these data, we concluded that, in our mouse model, the responsible $CD4^+$ T-cell subset in the induction site of AIH is T_{FH} cells.

Previously, we reported that severely inflamed livers in 3-week-old NTx-PD-$1^{-/-}$ mice contained a massive infiltration of activated $CD4^+$ and $CD8^+$ T cells producing inflammatory cytokines, such as IFN-γ and tumor necrosis factor-α.[3] In contrast, we found in this study that in the induction phase of AIH, IL-21-producing splenic T_{FH} cells were responsible for the initiation of liver inflammation. Thus, dysregulated T_{FH} cells and Th1-like cells appear to operate at different time points in the development of fatal AIH. Recent studies show that, although in experimental autoimmune encephalomyelitis (EAE), a $CD4^+$ T cell–mediated disease of the central nervous system, Th1 cells are present in EAE lesions during its active phase, and, in its induction phase, Th17 cells directly initiate inflammation and trigger the entry of a second wave of Th1 cells that migrate into the EAE lesions.[13] Because we found up-regulation of bcl-6 and t-bet in both splenic and hepatic $CD4^+$ T cells of 3-week-old NTx-PD-$1^{-/-}$ mice, it might be that, in the progression phase of AIH, dysregulated T_{FH} cells directly differentiate into Th1-like cells in the spleen and give rise to the migration of a second wave of Th1-like cells into the liver.

In this mouse model, infiltration of both $CD4^+$ and $CD8^+$ T cells in the liver are required for progression to fatal AIH, and the infiltration of $CD8^+$ T cells in the liver depends on $CD4^+$ T cells. In the induction phase of AIH, splenic $CD8^+$ T cells showed Ki-67^{high} activated T-cell phenotype. $CD4^+$ T cells from the spleen of 2-week-old NTx-PD-$1^{-/-}$ mice induced IL-21-driven $CD8^+$ T-cell activation. In addition, activated $CD8^+$ T cells in the spleen expressed CCR6 and were preferentially recruited to the liver via CCL20. However, the precise roles of $CD8^+$ T cells in the induction phase of AIH are still unclear. Because a large number of $CD8^+$ T cells infiltrated into the liver during AIH progression, $CD8^+$ T cells infiltrated in the induction phase might be involved in triggering the subsequent expansion and/or infiltration of inflammatory T cells in the progression phase.

We showed here that the CCR6-CCL20 axis is essential for splenic T_{FH} cells to migrate into the liver, triggering inflammation. CCR6 is also expressed on Th17 cells and is vital to the initiation of Th17-cell migration to target tissues.[13-15] CCR6 is expressed on not only Th17 cells but also Tregs in mice[14,15] and human T cells that produce both IL-17 and IFN-γ as well as Th1 cells.[16] Taken together, these data suggest that the CCR6-CCL20 axis plays an important role in the migration of instructed $CD4^+$ T cells into target tissues.

We also showed that NTx-PD-$1^{-/-}$ mice but not NTx mice at 2 weeks generated T_{FH} cells in the spleen. In addition, concomitant administration of blocking mAbs to PD-L1 and PD-L2 generated T_{FH} cells in the spleen of NTx mice at 2 weeks. Moreover, purified $CD4^+$ T cells in the spleen of 1-week-old NTx-PD-$1^{-/-}$ mice had greater IL-21 mRNA expression than those in NTx mice. In this regard, recent studies suggested that PD-1 deficiency increased T_{FH}-cell numbers but reduced IL-21 production by T_{FH} cells in long-term humoral immunity[17] and that T_{FH}-cell differentiation requires strong signals through the T-cell receptor.[18] Thus, in our model, PD-1 deficiency may induce enhanced production of IL-21 by activated autoreactive $CD4^+$ T cells to differentiate into T_{FH} cells in the induction phase. On the other hand, we found that PD-L1 but not PD-L2 mRNA expression was up-regulated in the liver of NTx-PD-$1^{-/-}$ mice. Because PD-1 and PD-1 ligands expressions are increased in the livers of most AIH patients,[19,20] it is possible that PD-1/PD-L1 interaction is insufficient to completely suppress liver inflammation but may halt progression to fatal AIH.

In humans, it is unknown at present whether the spleen is the induction site of AIH or T_{FH} cells are the T-cell subset responsible for induction of AIH. In patients with active AIH, splenomegaly is a common clinical finding. However, splenectomy for these patients has not been reported to be therapeutic. Therefore, splenectomy may help patients at the early phase of AIH but not those with more advanced cases. Notably, because patients with severe AIH have a high potential for recurrence after liver transplantation and the recurrence of AIH leads to a greater probability of graft loss,[21,22] splenectomy might be a therapeutic option to prevent recurrence after liver transplantation. On the other hand, it may be that dysregulated T_{FH} cells are involved in both B cell- and T cell–mediated autoimmunity in human AIH. Indeed, T_{FH} cells not only offer powerful help to B cells in forming germinal centers in humoral immunity but also induce B cell–mediated systemic autoimmunity in humans and mice.[7-9,23] In addition, although T_{FH} cells are mainly localized in B-cell follicles in lymphoid organs, circulating T cells resembling T_{FH} cells exist in the peripheral blood of patients with systemic lupus erythematosus.[10]

Furthermore, IL-21 secreted by effecter T cells including T_{FH} cells can modulate the activity of $CD8^+$ T cells and other immune and nonimmune cells in humans and mice.[11]

In conclusion, we demonstrated in the present study that Tregs and PD-1–mediated signaling are important in regulating T_{FH} cells and that dysregulated T_{FH} cells in the spleen are responsible for induction of fatal AIH in NTx-PD-$1^{-/-}$ mice. In addition, CCR6-CCL20 axis-dependent migration of T_{FH} cells is crucial for initiation of AIH. These data may lead to novel therapeutic approaches to human AIH, especially acute-onset fulminant AIH.

Supplementary Material

Note: To access the supplementary material accompanying this article, visit the online version of *Gastroenterology* at www.gastrojournal.org, and at doi: 10.1053/j.gastro.2011.01.002.

References

1. Krawitt EL. Autoimmune hepatitis. N Engl J Med 2006;354: 54–66.
2. Manns MP, Vogel A. Autoimmune hepatitis, from mechanisms to therapy. Hepatology 2006;43:S132–S144.
3. Kido M, Watanabe N, Okazaki T, et al. Fatal autoimmune hepatitis induced by concurrent loss of naturally arising regulatory T cells and PD-1-mediated signaling. Gastroenterology 2008;135:1333–1343.
4. Diamantis I, Boumpas DT. Autoimmune hepatitis: evolving concepts. Autoimmun Rev 2004;3:207–214.
5. Ichiki Y, Aoki CA, Bowlus CL, et al. T cell immunity in autoimmune hepatitis. Autoimmun Rev 2005;4:315–321.
6. Suzuki Y, Kobayashi M, Hosaka T, et al. Peripheral CD8+/CD25+ lymphocytes may be implicated in hepatocellular injuries in patients with acute-onset autoimmune hepatitis. J Gastroenterol 2004;39:649–653.
7. McHeyzer-Williams LJ, Pelletier N, Mark L, et al. Follicular helper T cells as cognate regulators of B cell immunity. Curr Opin Immunol 2009;21:266–273.
8. King C. New insights into the differentiation and function of T follicular helper cells. Nat Rev Immunol 2009;9:757–766.
9. Yu D, Batten M, Mackay CR, et al. Lineage specification and heterogeneity of T follicular helper cells. Curr Opin Immunol 2009;21:619–625.
10. Simpson N, Gatenby PA, Wilson A, et al. Expansion of circulating T cells resembling follicular helper T cells is a fixed phenotype that identifies a subset of severe systematic lupus erythematosus. Arthritis Rheum 2010;62:234–244.
11. Monteleone G, Pallone F, Macdonald TT. Interleukin-21 (IL-21)-mediated pathways in T cell-mediated disease. Cytokine Growth Factor Rev 2009;20:185–191.
12. Korn T, Bettelli E, Oukka M, et al. IL-17 and Th17 cells. Annu Rev Immunol 2009;27:485–517.
13. Reboldi A, Coisne C, Baumjohann D, et al. C-C chemokine receptor 6-regulated entry of TH-17 cells into the CNS through the choroid plexus is required for the initiation of EAE. Nat Immunol 2009;10:514–523.
14. Hirota K, Yoshitomi H, Hashimoto M, et al. Preferential recruitment of CCR6-expressing Th17 cells to inflamed joints via CCL20 in rheumatoid arthritis and its animal model. J Exp Med 2007; 204:2803–2812.
15. Yamazaki T, Yang XO, Chung Y, et al. CCR6 regulates the migration of inflammatory and regulatory T cells. J Immunol 2008;181: 8391–8401.
16. Acosta-Rodriguez EV, Rivino L, Geginat J, et al. Surface phenotype and antigenic specificity of human interleukin 17-producing T helper memory cells. Nat Immunol 2007;8:639–646.
17. Good-Jacobson KL, Szumilas CG, Chen L, et al. PD-1 regulates germinal center B cell survival and the formation and affinity of long-lived plasma cells. Nat Immunol 2010;11:535–542.
18. Fazilleau N, McHeyzer-Williams LJ, Rosen H, et al. The function of follicular helper T cells is regulated by the strength of T cell antigen receptor binding. Nat Immunol 2009;10:375–384.
19. Oikawa T, Takahashi H, Ishikawa T, et al. Intrahepatic expression of the co-stimulatory molecules programmed death-1, and its ligands in autoimmune liver disease. Pathol Int 2007;57:485–492.
20. Kassel R, Cruise MW, Iezzoni JC, et al. Chronically inflamed livers up-regulate expression of inhibitory B7 family members. Hepatology 2009;50:1625–1637.
21. Vogel A, Heinrich E, Bahr MJ, et al. Long-term outcome of liver transplantation for autoimmune hepatitis. Clin Transplant 2004; 18:62–69.
22. Rowe IA, Webb K, Gunson BK, et al. The impact of disease recurrence on graft survival following liver transplantation: a single centre experience. Transpl Int 2008;21:459–465.
23. Linterman MA, Rigby RJ, Wong RK, et al. Follicular helper T cells are required for systemic autoimmunity. J Exp Med 2009;206: 561–576.

Received June 4, 2010. Accepted January 10, 2011.

Reprint requests

Address requests for reprints to: Norihiko Watanabe, MD, PhD, Department of Gastroenterology and Hepatology, Graduate School of Medicine, Kyoto University, Kyoto 606-8501, Japan. e-mail: norihiko@kuhp.kyoto-u.ac.jp; fax: (81) 75-751-4303.

Acknowledgments

The authors thank Dr Dovie Wylie for assistance in preparation of the manuscript; Chigusa Tanaka for excellent technical assistance; and Drs Tasuku Honjo, Shuh Narumiya, Nagahiro Minato, Shimon Sakaguchi, and Ichiro Aramori for critical discussion and suggestions.

N.A. and M.K. contributed equally to this work.

Conflicts of interest

The authors disclose no conflicts.

Funding

Support for the Center for Innovation in Immunoregulative Technology and Therapeutics is provided in part by the Special Coordination Funds for Promoting Science and Technology of the Japanese Government and in part by Astellas Pharma Inc in the Formation of Innovation Center for Fusion of Advanced Technologies Program.

Supplementary Materials and Methods

Mice

BALB/c mice were purchased from Japan SLC (Shizuoka, Japan), and programmed cell death 1 (PD-1)$^{-/-}$ and RAG2$^{-/-}$ mice on a BALB/c background were generated as described.[1,2] All of these mice were bred and housed under specific pathogen-free conditions. Thymectomy and splenectomy of the mice 3 days after birth were performed as described.[3,4] All mouse protocols were approved by the Institute of Laboratory Animals, Graduate School of Medicine, Kyoto University.

Enzyme-Linked Immunosorbent Assay

Serum immunoglobulin (Ig) levels were determined by enzyme-linked immunosorbent assay (ELISA) as described,[5] and antibody (Ab) sets for detection of mouse IgG1, IgG2a, IgG2b, IgG3, IgA, and IgE from BD Biosciences (San Jose, CA) and anti-mouse IgM from AbD Serotec (Oxford, UK) were used. To detect serum antinuclear antibody (ANA), microtiter plates (Nunc, Roskilde, Denmark) were incubated with 10 μg/mL antigens, and the nuclear fraction was prepared from normal liver.[6] Ab sets for detection of mouse ANA subclasses were the same as above.

Administration of Abs in Vivo

PD-1–deficient BALB/c mice thymectomized 3 days after birth (NTx-PD-1$^{-/-}$ mice) at 1 day after thymectomy were intraperitoneally injected every week with 100 μg of Abs. Anti-CD4 (RM4-5) and anti-CD8 (53-6.7) for depletion of CD4$^+$ T cells and CD8$^+$ T cells, respectively, and neutralizing Abs to mouse inducible costimulator (ICOS) (7E.17G9) were from eBioscience (San Diego, CA). Neutralizing Abs to mouse interleukin (IL)-21 (AF594) and IL-12p40 (C17.8) as well as CCL20 (114908) were from R&D Systems (Minneapolis, MN). Neutralizing Abs to mouse PD-L1 and PD-L2 were purified from ascites as described.[7] All isotypes were from eBioscience or R&D Systems (Minneapolis, MN). After 2 to 4 injections, mice at 2 to 4 weeks of age were killed, and their spleens and livers were harvested.

Histologic and Immunohistologic Analysis

Organs were fixed in neutral buffered formalin and embedded in paraffin wax. Sections were stained with H&E for histopathology. Fluorescence immunohistology was performed on frozen sections as described previously[3] using fluorescein isothiocyanate (FITC)-conjugated anti-CD4 (RM4-5), anti-CD8a (Ly-2) (eBioscience), peanut agglutinin (PNA; Vector Laboratories, Burlingame, CA), and biotin-labeled anti-B220 (RA3-6B2) (BD Biosciences) followed by Texas red-conjugated avidin (Vector Laboratories). Numbers of CD4$^+$ T cells localized within B220$^+$ B-cell follicles in the spleen and inflamed liver were counted in several high-power fields in at least 3 sections of each mouse. Diameter of germinal center (GC) was measured in several high-power fields in at least 3 sections of each mouse. Single-cell suspensions of isolated splenic CD4$^+$ICOS$^+$ T cells from 2.5-week-old NTx-PD-1$^{-/-}$ mice were mounted on glass slides by cytocentrifuge preparation. After fixation, these cells were stained with anti-Bcl6 (N3) (Santa Cruz Biotechnology, Santa Cruz, CA) followed by FITC-conjugated goat anti-rabbit Ig (BD Biosciences) or anti–IL-21 (AF594) (R&D Systems) followed by FITC-conjugated rabbit anti-goat Ig (ab6737) (Abcam, Cambridge, MA), and DAPI (Sigma-Aldrich, St. Louis, MO). Rabbit IgG isotype (DA1E) and normal goat IgG isotype (AB-108-C) were from Cell Signaling (Danvers, MA) and from R&D Systems, respectively.

Flow Cytometry Analysis and Isolation of Lymphocytes

Single cells from the livers and spleens were prepared as described.[3] The following mAbs were used for staining: FITC-conjugated anti-CD3e (145-2C11), anti-CD8a (eBioscience); anti-CXCR5 (2G8), anti-GL7, anti-Ki67 (B56) (BD Biosciences); PE-conjugated anti-CD3e, anti-CD4, anti-CD25 (PC61.5), anti-ICOS (eBioscience); anti-B220, anti-CD95/Fas (Jo2) (BD Biosciences); anti-CCR6 (140706), anti-CCR9 (242503), anti-CXCR3 (220803) (R&D Systems); APC-Cy7-conjugated anti-CD4 (GK1.5), biotin-labeled B220 (BD Biosciences); and allophycocyanin (APC)-conjugated streptavidin, and anti-CD8a (eBioscience). In flow cytometric analysis of CD4$^+$ T cells and B220$^+$ B cells in Figure 3, cells were stained with FITC-anti-CXCR5, PE-anti-ICOS, and APC-Cy7-anti-CD4 for CD4$^+$ T cells, or with FITC-anti-GL7, PE-anti-CD95/Fas, and biotin-labeled B220 followed by APC-conjugated streptavidin for B220$^+$ B cells. For Ki-67 antigen staining in Figure 5, a FITC-conjugated Ab set (BD Bioscience) was used with PE-anti-CD3 and APC-Cy7-anti-CD4 or APC-anti-CD8. In flow cytometric analysis of T cells in Figure 6, cells were stained with FITC-anti-CD3e, PE-anti-CCR6, -anti-CCR9, or -anti-CXCR3 and APC-Cy7-anti-CD4, with FITC-anti-CXCR5, PE-anti-CCR6, and APC-Cy7-anti-CD4, or with FITC-anti-CD3e, PE-anti-CCR6, and APC-anti-CD8. Stained cells were analyzed with a FACSCanto II (BD Biosciences). Data were analyzed using Cell Quest Pro (BD Biosciences). Dead cells were excluded on the basis of side- and forward-scatter characteristics, and viable T-cell numbers were calculated as follows: (the percentage of cells in the cell type) $\times$ (the number of viable cells). CD3$^+$CD4$^+$, CD3$^+$CD8$^+$, CD3$^-$B220$^+$ cells from the spleen or liver, and CD4$^+$ICOS$^+$, CD4$^+$ICOS$^-$ T cells and CD4$^+$CD25$^+$ T regulatory cells (Tregs) from the spleen were obtained by a FACS Aria II (BD Biosciences) to reach >99% purity, as described.[3]

Adoptive Transfer

$CD4^+CD25^+$ Tregs were prepared from the spleen of adult BALB/c PD-$1^{+/+}$ or PD-$1^{-/-}$ mice as described.[3] Tregs (1×10^6) were intraperitoneally injected into NTx-PD-$1^{-/-}$ mice at 1 day after thymectomy. For transfer of follicular helper T (T_{FH}) cells or non-T_{FH} cells, $CD4^+ICOS^+$ T cells or $CD4^+ICOS^-$ T cells, respectively, were prepared from the spleen of 2.5-week-old NTx-PD-$1^{-/-}$ mice as described above. Isolated T cells (1×10^6) were intravenously injected into RAG2-deficient recipient mice on a BALB/c background at 4 weeks of age. Three weeks after transfer, recipient mice were examined.

Real-Time Quantitative Reverse-Transcription Polymerase Chain Reaction

Real-time quantitative reverse-transcription polymerase chain reaction was performed as described previously.[8] Spleen and liver tissues or isolated lymphocytes were frozen in RNA later. RNA was prepared with an RNeasy mini kit (Qiagen, Hilden, Germany), and single-strand complementary DNA (cDNA) was synthesized with SuperScript II reverse transcriptase (Invitrogen, Carlsbad, CA). Real-time quantitative reverse-transcription polymerase chain reaction was performed using SYBR Green I Master (Roche Applied Science, Basel, Switzerland). The real-time quantitative reactions were performed using a Light Cycler 480 (Roche Applied Science) according to the manufacturer's instructions. Values are expressed as arbitrary units relative to glyceraldehyde-3-phosphate dehydrogenase (GAPDH). The following primers were used: *GAPDH*: 5′-CAACTTTGTCA AGCTCATTTCC-3′ and 5′-GGTCCAGGGTTTCTTA CTCC-3′; *PD-L1*: 5′-GGAATTGTCTCAGAATGGTC-3′ and 5′-GTAGTTGCTTCTAGGAAGGAG-3′; *PD-L2*: 5′-GCATGTTCTGGAATGCTCAC-3′ and 5′-CTTTGGGT TCCATCCGACT-3′; *Foxp3*: 5′-TCAGGAGCCCACC AGTACA-3′ and 5′-TCTGAAGGCAGAGTCAGGAGA-3′; *Bcl6*: 5′-ACACATGCAGGAAGTTCATCAAGG-3′ and 5′-CATATTGTTCTCCACGACCTCACG-3′; *IL-21*: 5′-GACATTCATCATCGACCTCGT-3′ and 5′-TCACAGG AAGGGCATTTAGC-3′; *IL-21R*: 5′-AGTGACCCCGTCAT CTTTCA-3′ and 5′-AGGAGCAGCAGCATGTGAG-3′; *RORγT*: 5′-CCGCTGAGAGGGCTTCAC-3′ and 5′-TG CAGGAGTAGGCCACATTACA-3′; *IL-17A*: 5′-CTCCA GAAGGCCCTCAGACTAC-3′ and 5′-AGCTTTCCCTC CGCATTGACACAG-5′; *T-bet*: 5′-TCAACCAGCACCAGA CAGAG-3′ and 5′-AAACATCCTGTAATGGCTTGTG-3′; *GATA-3*: 5′-TTATCAAGCCCAAGCGAAG-3′ and 5′-TG GTGGTGGTCTGACAGTTC-3′; *CCL20*: 5′-ATGGCCTG CGGTGGCAAGCGTCT-3′ and 5′-TAGGCTGAGGAG GTTCACAGCCC-3′; *CCL25*: 5′-GAGTGCCACCCTAG GTCATC-3′ and 5′-CCAGCTGGTGCTTACTCTGA-3′.

T-Cell Coculture

$CD4^+$ and $CD8^+$ T cells were isolated from the spleen of 2-week-old PD-$1^{-/-}$ mice with or without neonatal thymectomy (NTx) using a FACS Aria II (BD Biosciences) to reach >99% purity, as described.[3] Isolated $CD8^+$ T cells (5×10^5) were cocultured with 5×10^5 freshly isolated $CD4^+$ T cells in round-bottomed, 96-well culture plates in Dulbecco's modified Eagle medium supplemented with 10% fetal bovine serum, 50 mmol/L 2-mercaptoethanol, 100 U/mL penicillin, and 100 μg/mL streptomycin. In some experiments, we used the following reagents in these culture conditions: 10 μg/mL of anti-IL-21 (AF594), 10 μg/mL of goat IgG isotype, and 1–100 ng/mL of recombinant IL-21 (all from R&D Systems). After 24 hours of culture, cells were stained with PE-anti-CD3, APC-anti-CD8, and FITC-anti-Ki67 or -isotype control and analyzed with a FACSCanto II.

References

1. Nishimura H, Okazaki T, Tanaka Y, et al. Autoimmune dilated cardiomyopathy in PD-1 receptor-deficient mice. Science 2001; 291:319–322.
2. Shinkai Y, Rathbun G, Lam KP, et al. RAG-2-deficient mice lack mature lymphocytes owing to inability to initiate V(D)J rearrangement. Cell 1992;68:855–867.
3. Kido M, Watanabe N, Okazaki T, et al. Fatal autoimmune hepatitis induced by concurrent loss of naturally arising regulatory T cells and PD-1-mediated signaling. Gastroenterology 2008;135:1333–1343.
4. Klonowski KD, Marzo AL, Williams KJ, et al. CD8 T cell recall responses are regulated by the tissue tropism of the memory cell and pathogen. J Immunol 2006;177:6738–6746.
5. Muramatsu M, Kinoshita K, Fagarasan S, et al. Class switch recombination and hypermutation require activation-induced cytidine deaminase (AID), a potential RNA editing enzyme. Cell 2000; 102:553–563.
6. Blobel G, Potter VR. Nuclei from rat liver: isolation method that combines purity with high yield. Science 1966;154:1662–1665.
7. Ishida M, Iwai Y, Tanaka Y, et al. Differential expression of PD-L1 and PD-L2, ligands for an inhibitory receptor PD-1, in the cells of lymphohematopoietic tissues. Immunol Lett 2002;84:57–62.
8. Kido M, Tanaka J, Aoki N, et al. *Helicobacter pylori* promotes the production of thymic stromal lymphopoietin by gastric epithelial cells and induces dendritic cell-mediated inflammatory Th2 responses. Infect Immun 2010;78:108–114.

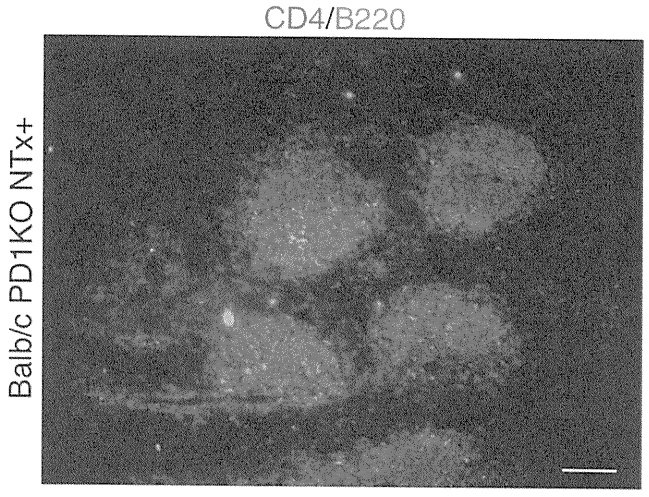

Supplementary Figure 1. Splenic CD4$^+$ T cells are preferentially localized within B220$^+$ B-cell follicles in the induction phase of AIH in NTx-PD-1$^{-/-}$ mice. The spleens from 2-week-old NTx-PD-1$^{-/-}$ mice were stained with biotin-labeled anti-B220 and FITC-conjugated anti-CD4 followed by Texas red-conjugated avidin. *Scale bar*, 100 μm.

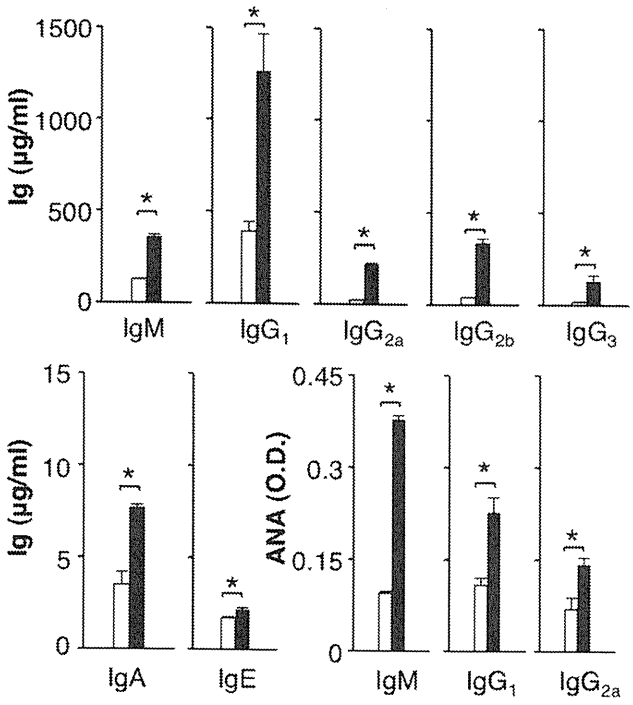

Supplementary Figure 3. Three-week-old NTx-PD-1$^{-/-}$ mice show hyper-γ-globulinemia and vast production of class-switched antinuclear antibodies (ANAs). The serum levels of total Ig subclasses and ANAs in IgM, IgG1, and IgG2a of 3-week-old PD-1$^{-/-}$ mice with (*solid columns*) or without (*open columns*) NTx determined by ELISA. *Bars* indicate the mean of each group, and *horizontal short bars* indicate the standard deviation. *$P < .05$.

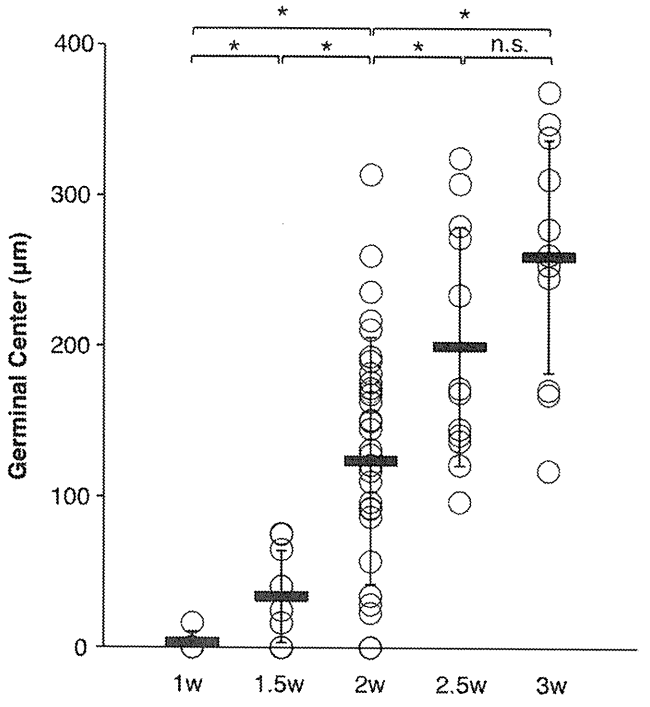

Supplementary Figure 2. The size of GCs is increased in the spleen of NTx-PD-1$^{-/-}$ mice from 1 to 3 weeks of age. Spleens from NTx-PD-1$^{-/-}$ mice at the indicated age in weeks were stained with FITC-conjugated PNA and biotin-labeled anti-B220 followed by Texas red-conjugated avidin. Each *open circle* represents a size of GC as measured in high-power fields. *Horizontal bars* indicate the mean size (diameter) of GCs in at least 3 sections. *Horizontal short bars* indicate the standard deviation. *$P < .05$.

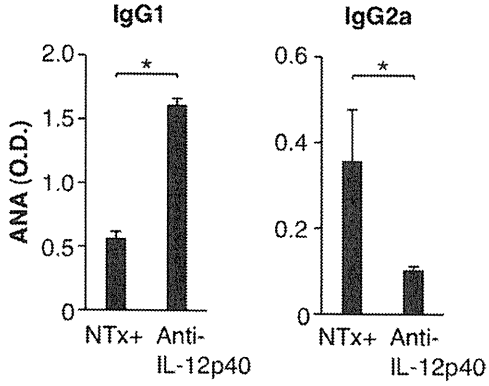

Supplementary Figure 4. Administration of anti–IL-12p40 induces increase of IgG1 and decrease of IgG2a classes of antinuclear antibodies (ANAs). NTx-PD-1$^{-/-}$ mice were injected intraperitoneally at 1 day after NTx and then once a week with anti–IL-12p40 (n = 5) Abs. After 4 injections, mice at 4 weeks of age were killed, and the serum levels of ANAs in IgG1 and IgG2a were determined by ELISA. *Bars* indicate the mean of NTx-PD-1$^{-/-}$ with or without administration of anti–IL-12p40, and *horizontal short bars* indicate the standard deviation. *$P < .05$.

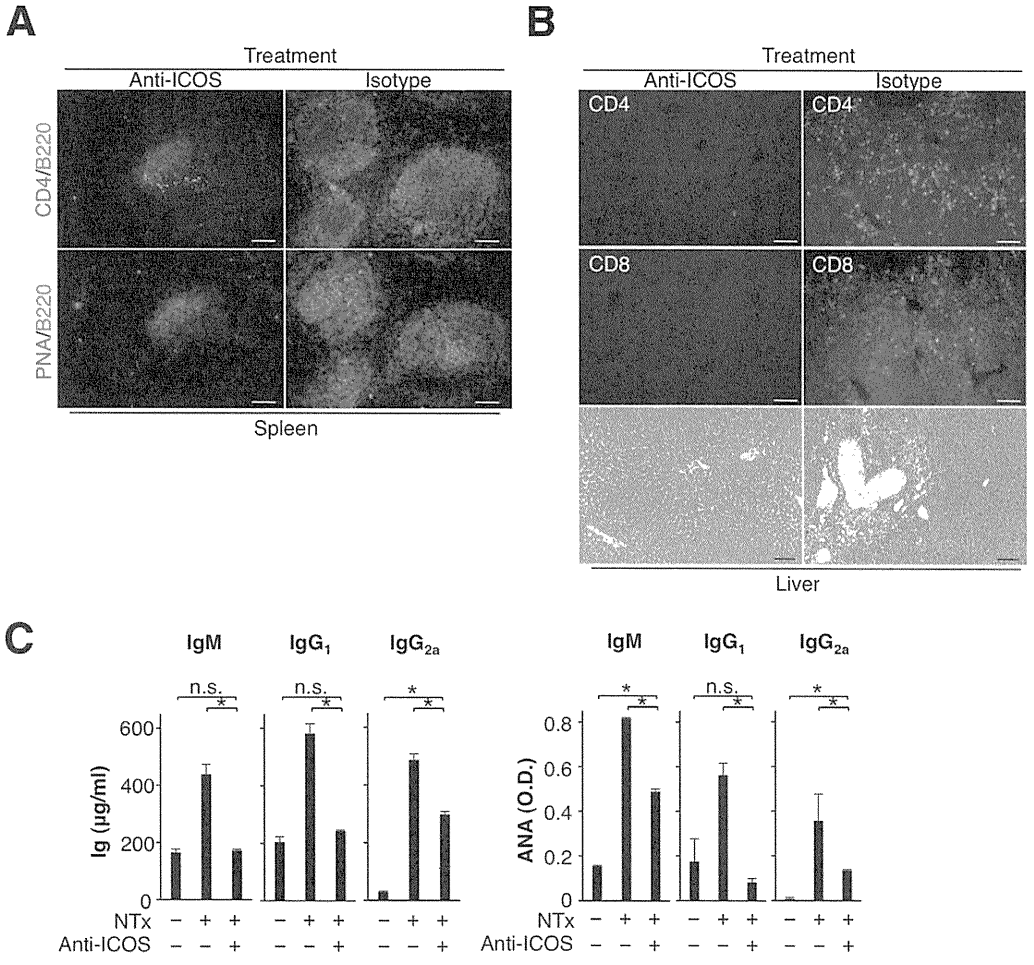

Supplementary Figure 5. Administration of anti-ICOS suppresses not only T_{FH}-cell generation but also induction of fatal AIH, including hyper-γ-globulinemia and vast production of class-switched anti-nuclear antibodies (ANAs). (*A–C*) NTx-PD-1$^{-/-}$ mice were injected intraperitoneally at 1 day after NTx and then once a week with either anti-ICOS (n = 5) or isotype (n = 7) Abs. After 4 injections, mice at 4 weeks of age were killed and the spleens and livers harvested. Double immunostainings of the spleen. (*A*) The spleens from indicated mice were stained with FITC-conjugated anti-CD4 or PNA (*green*) and biotin-labeled anti-B220 followed by Texas red-conjugated avidin (*red*). (*B*) Stainings of the liver for hematoxylin and eosin (*HE*), CD4, and CD8. (*C*) The serum levels of total Ig subclasses and ANAs in IgM, IgG1, and IgG2a were determined by ELISA. *Bars* indicate the mean of each group, and *horizontal short bars* indicate the standard deviation. *$P < .05$. All *scale bars*, 100 μm.

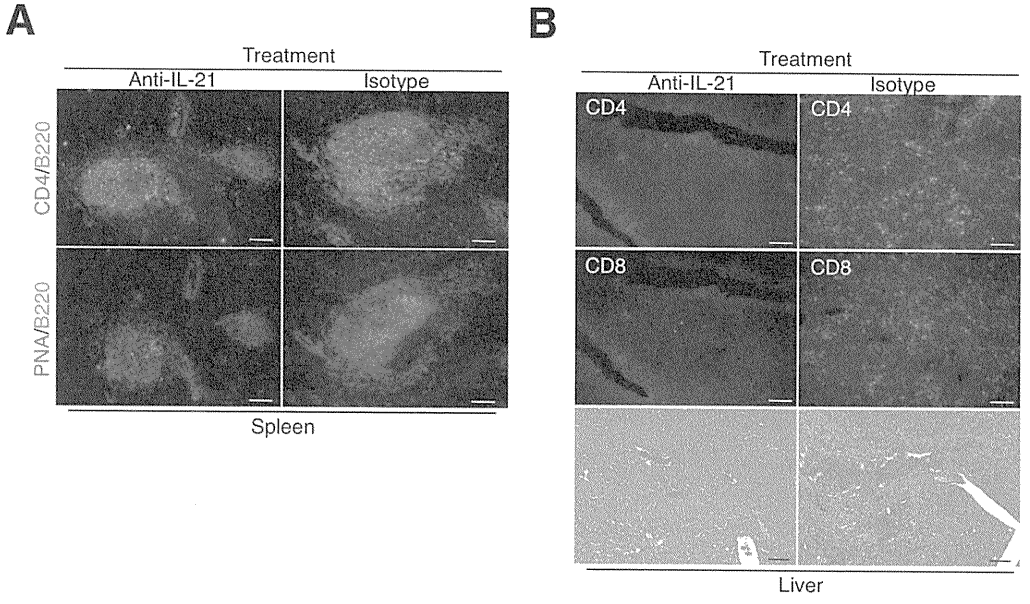

Supplementary Figure 6. Administration of anti–IL-21 suppresses not only T_{FH}-cell generation but also induction of fatal AIH. NTx-PD-$1^{-/-}$ mice were injected intraperitoneally at 1 day after NTx and then once a week with either anti–IL-21 (n = 5) or isotype (n = 5) Abs. After 4 injections, mice at 4 weeks of age were killed, and the spleens and livers were harvested. (*A*) Double immunostainings of the spleen. The spleens from indicated mice were stained with FITC-conjugated anti-CD4 or PNA (*green*) and biotin-labeled anti-B220 followed by Texas red-conjugated avidin (*red*). (*B*) Stainings of the liver for hematoxylin and eosin (*HE*), CD4, and CD8. All *scale bars*, 100 μm.

INFECTION AND IMMUNITY, Jan. 2010, p. 108–114
0019-9567/10/$12.00 doi:10.1128/IAI.00762-09

Vol. 78, No. 1

Helicobacter pylori Promotes the Production of Thymic Stromal Lymphopoietin by Gastric Epithelial Cells and Induces Dendritic Cell-Mediated Inflammatory Th2 Responses▽

Masahiro Kido,[1,2] Junya Tanaka,[1,2] Nobuhiro Aoki,[1,2] Satoru Iwamoto,[1,2] Hisayo Nishiura,[1,2] Tsutomu Chiba,[1] and Norihiko Watanabe[1,2]*

Department of Gastroenterology and Hepatology[1] and Center for Innovation in Immunoregulative Technology and Therapeutics,[2] Graduate School of Medicine, Kyoto University, Yoshida-Konoe-cho, Sakyo-ku, Kyoto 606-8501, Japan

Received 7 July 2009/Returned for modification 6 August 2009/Accepted 3 October 2009

***Helicobacter pylori* colonizes the stomach and induces strong, specific local and systemic humoral and cell-mediated immunity, resulting in the development of chronic gastritis in humans. Although *H. pylori*-induced chronic atrophic gastritis is characterized by marked infiltration of T helper type 1 (Th1) cytokine-producing CD4$^+$ T cells, almost all of the inflamed gastric mucosae also contain focal lymphoid aggregates with germinal centers. In addition, typical *H. pylori*-induced chronic gastritis in children, called follicular gastritis, is characterized by B-cell follicle formation in the gastric mucosa. The aim of this study was to examine whether thymic stromal lymphopoietin (TSLP), an epithelial-cell-derived cytokine inducing a dendritic cell (DC)-mediated inflammatory Th2 response, is involved in Th2 responses triggering B-cell activation in *H. pylori*-induced gastritis. Here, we show that *H. pylori* triggered human gastric epithelial cells to produce TSLP, together with the DC-attracting chemokine MIP-3α and the B-cell-activating factor BAFF. After DCs were incubated with supernatants from *H. pylori*-infected epithelial cells, the conditioned cells expressed high levels of costimulatory molecules, such as CD80, and triggered naïve CD4$^+$ T cells to produce high levels of the Th2 cytokines interleukin-4 and interleukin-13 and of the inflammatory cytokines tumor necrosis factor alpha and gamma interferon. In contrast, after incubation of the supernatants with the neutralizing antibodies to TSLP, the conditioned DCs did not prime T cells to produce high levels of Th2 cytokines. These results, together with the finding that TSLP was expressed by the epithelial cells of human follicular gastritis, suggest that *H. pylori* can directly trigger epithelial cells to produce TSLP. It also suggests that TSLP-mediated DC activation may be involved in Th2 responses triggering B-cell activation in *H. pylori*-induced gastritis.**

Helicobacter pylori (*H. pylori*) infection in the stomach induces chronic gastritis associated with the development of peptic ulcer diseases, gastric adenocarcinoma, and mucosa-associated lymphoid tissue (MALT) lymphoma in humans (3, 8, 35). Although *H. pylori*-induced chronic atrophic gastritis is characterized by marked infiltration of T helper type 1 (Th1) cytokine-producing CD4$^+$ T cells (3, 8, 35), almost all of the inflamed gastric mucosae also contain focal lymphoid aggregates with germinal centers (5, 11). In addition, typical *H. pylori*-induced chronic gastritis in children, called follicular gastritis, is characterized by B-cell follicle formation in the gastric mucosa (10, 11, 34). Th2 responses triggering B-cell activation appear to be involved in the development of lymphoid aggregates with germinal centers. However, molecular mechanisms to induce Th2 responses triggering B-cell activation are not clear.

In humans, an epithelial-cell-derived cytokine, thymic stromal lymphopoietin (TSLP), activates CD11c$^+$ myeloid dendritic cells (DCs), and activated DCs strongly upregulate the expression of costimulatory molecules, such as CD80 and CD86 (23, 38, 43, 44). TSLP-activated DCs promote CD4$^+$ T cells to differentiate into inflammatory Th2 cells that produce interleukin-4 (IL-4), IL-5, IL-13, and tumor necrosis factor alpha (TNF-α) while downregulating IL-10 and gamma interferon (IFN-γ) (23, 44). Interestingly, TSLP primes DCs to produce large amounts of IL-12 following CD40 ligand stimulation. In addition, DCs activated with TSLP and CD40 ligand induce the differentiation of naïve CD4$^+$ T cells into effectors producing both Th1 and Th2 cytokines. These findings suggest that IL-12-mediated negative regulation of Th2 responses is not effective in TSLP-induced Th2 inflammation and that it leads to a mixed Th1 and Th2 profile (42).

Here, we show that *H. pylori* triggered human gastric epithelial cells to produce TSLP. Such cells produced a DC-attracting chemokine, macrophage inflammatory protein 3α (MIP-3α), and a B-cell-activating factor belonging to the TNF family (BAFF). After DCs were incubated with supernatants from *H. pylori*-infected epithelial cells, the conditioned cells expressed high levels of costimulatory molecules and triggered naïve CD4$^+$ T cells to produce IL-4 and IL-13 with the inflammatory cytokines TNF-α and IFN-γ. In addition, TSLP was expressed by the epithelial cells of human follicular gastritis. These results suggest that *H. pylori* can directly trigger epithelial cells to produce TSLP and that TSLP-mediated DC activation may be involved in Th2 responses triggering B-cell activation in *H. pylori*-induced gastritis.

* Corresponding author. Mailing address: Department of Gastroenterology and Hepatology, Kyoto University, Yoshida-Konoe-cho, Sakyo-ku, Kyoto 606-8501, Japan. Phone: 81-75-751-4319. Fax: 81-75-751-4303. E-mail: norihiko@kuhp.kyoto-u.ac.jp.

▽ Published ahead of print on 19 October 2009.

MATERIALS AND METHODS

***H. pylori* and *H. felis*.** *H. pylori* TN2GF4, isolated from a Japanese patient with a duodenal ulcer, was donated by M. Nakao (Pharmaceutical Research Division, Takeda Chemical Industries, Ltd., Osaka, Japan). It was maintained as described previously (26). The inoculated *H. pylori* strain, TN2GF4, was CagA and VacA positive, as described previously (46). *Helicobacter felis* (ATCC 49179) was purchased from the American Type Culture Collection (Rockville, MD). The bacteria were grown in brucella broth at a titer of 1×10^8 organisms/ml. The bacterial suspension was stored at −80°C until it was used.

Gastric epithelial cell culture. Upon 80% confluence of the human gastric cancer cell line passages 20 to 30, AGS, MKN28, MKN45, MKN74, and KATOIII cells were trypsinized (trypsinethylenediaminetetraacetic acid; Gibco, Taastrup, Denmark). These cells were reseeded at 5.0×10^5 cells per well in six-well plates and maintained in RPMI 1640 medium (Gibco BRL, Grand Island, NY) supplemented with 10% (vol/vol) heat-inactivated fetal calf serum (Sigma, St. Louis, MO), penicillin G, and streptomycin (Gibco). Six hours after being seeded, the cells were washed with phosphate-buffered saline (PBS) and stimulated for 12 to 36 h in the presence of live *H. pylori* or *H. felis* at 1 cell per 150 bacteria or at the indicated cell/bacterium ratio. In some experiments, cells were stimulated with lipopolysaccharide (LPS) from *Escherichia coli* (1 μg/ml; Sigma) and cultured in a Transwell (Corning, NY).

Real-time quantitative RT-PCR. Real-time quantitative reverse transcription (RT)-PCR was performed as described previously (45). Gastric epithelial cells were frozen in RNAlater (Qiagen, Valencia, CA) and stored at −80°C until they were used. Total RNA was extracted using an RNeasy minikit (Qiagen) according to the manufacturer's instructions. Single-stranded cDNA was synthesized with SuperScript II reverse transcriptase (Invitrogen, Carlsbad, CA). Real-time quantitative reactions were performed with an ABI Prism 7300 detection system (Applied Biosystems, Foster City, CA) according to the manufacturer's instructions. Values are expressed as arbitrary units relative to glyceraldehyde-3-phosphate dehydrogenase (GAPDH). The following primers were used: GAPDH, 5′-CCACATCGCTCAGACACCAT-3′ and 5′-GGCAACAATATCCACTTTACCAGAGT-3′; TSLP, 5′-CCCAGGCTATTCGGAAACTCAG-3′ and 5′-CGCCACAATCCTTGTAATTGTG-3′ ; and BAFF, 5′-ACCGCGGGACTGAAAATCT-3′ and 5′-CACGCTTATTTCTGCTGTTCTGA-3′.

Cytokine production. After 24 h of culture of gastric epithelial cells under the conditions described above, culture supernatants were collected and analyzed with protein enzyme-linked immunosorbent assay (ELISA) kits for TSLP, MIP-3α, MIP-1α, MIP-1β, and monocyte chemoattractant protein 1 (MCP-1) (all from R&D Systems).

DC purification and culture. This study was approved by the Institutional Review Board for Human Research at the Graduate School of Medicine, Kyoto University. Peripheral blood mononuclear cells (PBMCs) were obtained from adult buffy coats of healthy donors (kindly provided by the Kyoto Red Cross Blood Center, Kyoto, Japan). $CD11c^+$ DCs were isolated from PBMCs as described previously (43). $CD11c^+$ $lineage^-$ cells were isolated with a FACS Aria (BD Biosciences, San Jose, CA) to >99% purity. $CD11c^+$ DCs were cultured immediately after being sorted in RPMI 1640 medium supplemented with 5% human AB serum (Sigma), penicillin G, streptomycin, 10 mM HEPES, and 1 mM sodium pyruvate (Gibco BRL) (referred to as complete medium). Cells were seeded at a density of 1×10^6/ml in round-bottom 96-well plates in the presence of 15 ng/ml of TSLP (R&D Systems, Minneapolis, MN) or 50 μl of supernatant from the *Helicobacter*-colonized gastric epithelial cells. For neutralization of TSLP, supernatants from *H. pylori*-colonized gastric epithelial cells were incubated with 20 μg/ml of anti-human TSLP (R&D Systems). After 24 h of culture, viable DCs were counted by trypan blue exclusion of dead cells.

Analysis of cell surface markers of DCs. To determine the cell surface markers characteristic of activated DCs, DCs were incubated with various stimuli for 24 h. The DCs were subsequently stained with fluorescein isothiocyanate (FITC)-conjugated anti-CD80 (Immunotech). Finally, they were analyzed with a FACS Calibur (BD Biosciences).

DC–T-cell coculture. After 24 h of culture, $CD11c^+$ DCs were collected and washed three times to remove any cytokines. Viable DCs were counted by trypan blue exclusion of dead cells. $CD4^+$ $CD45RA^+$ naive T cells were isolated from PBMCs using a FACS Aria to reach >99% purity, as described previously (43). The remaining DCs were cocultured with 2.5×10^4 freshly purified allogeneic naive $CD4^+$ T cells in round-bottom 96-well culture plates in complete medium. The cells were cultured in triplicate at a DC/T-cell ratio of 1:5. After 7 days of culture, viable cells were counted by trypan blue exclusion of dead cells.

T-cell cytokine production. DC-primed $CD4^+$ T cells were collected on day 7 of the coculture, washed twice, and restimulated with 50 ng/ml phorbol myristate acetate (PMA) (Sigma) plus 2 μg/ml ionomycin (Sigma) in flat-bottom 96- or 48-well plates at a concentration of 1×10^6 cells/ml. After 3.5 h, brefeldin A (Sigma) was added at 10 μg/ml. After 2.5 h, cells were collected and stained for cell surface molecules. The cells were fixed and permeabilized using a Fix & Perm Cell Permeabilization Kit (Caltag Laboratories, An Der Grub, Austria) and stained with phycoerythrin-conjugated monoclonal antibodies (MAbs) to IL-4, IL-13, TNF-α, and FITC-conjugated anti-IFN-γ (all from eBioscience). The stained cells were analyzed on a FACS Calibur.

Gastric mucosa samples. Samples of mucosa in biopsy specimens were obtained from inflamed gastric mucosae in three patients with *Helicobacter*-induced follicular gastritis (male/female ratio, 1/2; mean age [range], 37.3 [32–44] years). Samples of healthy controls were taken from three patients with duodenal ulcers (male/female ratio, 2/1; mean age [range], 37.7 [35–43] years) in whom the absence of inflammation had been histopathologically confirmed.

Histological and immunohistological analyses. Samples of mucosa in biopsy specimens were fixed in neutral buffered formalin and embedded in paraffin wax. Sections were stained with hematoxylin and eosin for histopathology. Fluorescence immunohistology was performed on frozen sections as described previously (18, 43, 45). In brief, 6-μm sections were cut from tissue blocks of frozen mucosal samples onto glass slides. The sections were air dried for 30 min, fixed in acetone for 5 min, and blocked with phosphate-buffered saline containing 10% nonfat dried milk for 30 min. The sections were stained with anti-human TSLP (43, 45), anti-CD11c (BD Pharmingen), or anti-DC-LAMP (Immunotech) antibodies (Abs) for 1 h, followed by staining using FITC-conjugated anti-immunoglobulin Abs. After the final wash, the slides were mounted with Vectashield (Vector Laboratories, Burlingame, CA) and examined under a fluorescence microscope.

Statistical analysis. Statistical analysis was performed by the Student *t* test for pairwise comparisons and analysis of variance with the Tukey-Kramer test for multiple comparisons. *P* values below 0.05 were considered significant.

RESULTS

***H. pylori* colonization induces TSLP expression in human gastric epithelial cells.** To test whether *H. pylori* colonization can induce expression of TSLP in gastric epithelial cells, various human gastric epithelial cell lines, such as AGS, MKN28, MKN45, MKN74, and KATOIII cells, were cultured for 24 h with *H. pylori*. Expression levels of mRNA encoding TSLP were measured using real-time quantitative RT-PCR. In contrast to the gastric epithelial cells not exposed to *H. pylori*, gastric epithelial cells—MKN28, MKN45, and MKN74—upregulated TSLP expression after *H. pylori* colonization (Fig. 1A). TSLP expression enhanced by *H. pylori* colonization was detectable when we used low epithelial cell/bacterium ratios (e.g., 1 cell per 70 to 100 bacteria) (Fig. 1B); it reached a maximal level at 1 cell per 150 to 200 bacteria and did not increase at ratios of 1 cell per 300 bacteria or higher. Because 150 to 200 bacteria can actually adhere to gastric epithelial cell membranes (6), the condition of epithelial cells expressing TSLP by *H. pylori* might be similar to mucosal lesions of *H. pylori*-infected gastritis patients. Next, we investigated the time course of *H. pylori*-induced TSLP expression (Fig. 1C). Upregulation of TSLP expression was induced after 12 h of *H. pylori* colonization and was sustained after 24 h of colonization.

Direct contact of *H. pylori* triggers human gastric epithelial cells to produce TSLP. *H. felis* is a gastric *Helicobacter* that colonizes the stomachs of laboratory mice, dogs, and cats and can induce active chronic gastritis that mimics the pathological features observed in *H. pyroli*-induced gastritis in humans (4, 9, 19, 20, 29). Next, we examined whether *H. felis* colonization can induce expression of TSLP in gastric epithelial cells. MKN28 and MKN45 cells were cultured for 24 h with *Helicobacter* bacteria, and the expression levels of mRNA encoding TSLP were measured using real-time quantitative RT-PCR. TSLP cytokine production in the culture supernatant was as-